Selection constrains phenotypic evolution in a functionally important plant trait

Christopher D. Muir[1]

[1]Biodiversity Research Centre and Botany Department, University of British Columbia,

Vancouver, British Columbia, Canada

6270 University Blvd.

Vancouver, BC, Canada V6T 1Z4

E-mail: cdmuir@biodiversity.ubc.ca

Phone: (778) 228-4851

Keywords: Adaptive landscape | phenotypic constraint | stomata | amphistomy | phylogenetic comparative methods

Abstract

A long-standing idea is that the macroevolutionary adaptive landscape – a 'map' of phenotype to fitness – constrains evolution because certain phenotypes are fit, while others are universally unfit. Such constraints should be evident in traits that, across many species, cluster around particular modal values, with few intermediates between modes. Here, I compile a new global database of 599 species from 94 plant families showing that stomatal ratio, an important functional trait affecting photosynthesis, is multimodal, hinting at distinct peaks in the adaptive landscape. The dataset confirms that most plants have all their stomata on the lower leaf surface (hypostomy), but shows for the first time that species with roughly half their stomata on each leaf surface (amphistomy) form a distinct mode in the trait distribution. Based on a new evolutionary process model, this multimodal pattern is unlikely without constraint. Further, multimodality has evolved repeatedly across disparate families, evincing long-term constraint on the adaptive landscape. A simple cost-benefit model of stomatal ratio demonstrates that selection alone is sufficient to generate an adaptive landscape with multiple peaks. Finally, phylogenetic comparative methods indicate that life history evolution drives shifts between peaks. This implies that the adaptive benefit conferred by amphistomy – increased photosynthesis – is most important in plants with fast life histories, challenging existing ideas that amphistomy is an adaptation to thick leaves and open habitats. I conclude that peaks in the adaptive landscape have been constrained by selection over much of land plant evolution, leading to predictable, repeatable patterns of evolution.

The topography of the macroevolutionary adaptive landscape is thought to shape the broad patterns of life's diversity [1]. Adaptive landscapes with multiple peaks are manifest in convergent evolution of similar phenotypes across independent evolutionary lineages. In such cases, surveys across species should reveal a multimodal trait distribution in which the modes point to the underlying peaks in the landscape. Multimodality has been observed frequently among plants and animals, including traits such as self-incompatibility [2], the precocial-altricial spectrum [3], pollination syndromes [4], ecomorphology in *Anolis* [5], and plant height [6]. That such disparate classes of traits show broadly similar patterns suggests that divergence on a multi-peaked adaptive landscape may be a general feature of macroevolution. However, we rarely know whether multimodality reflects constraints imposed by the underlying adaptive landscape and not some other constraint on phenotypic evolution.

In particular, certain phenotypes may be common not because they are more fit, but rather because they are genetically, developmentally, or functionally accessible. Conversely, rare phenotypes might be inaccessible. I use the definitions given by Arnold [7]: genetic constraints are limitations set by the "pattern of genetic variation and covariation for a set of traits"; developmental constraints are limitations on "possible developmental states"; and functional constraints are imposed by "time, energy, or the laws of physics". Arnold contrasts these with selective constraints determined by the adaptive landscape. There are examples of genetic [8], developmental [9], and functional [10] constraints on phenotypic evolution acting in nature, meaning that we cannot assume selection alone shapes trait evolution. Compelling evidence from cross species comparisons that selection constrains phenotypic evolution requires showing that phenotypic evolution is constrained, that selection is sufficient to explain the inferred constraint, and that nonselective constraints are inconsistent

3

26 with these observations.

27 Here, I evaluate evidence for selective constraints on a functionally important plant
28 trait, stomatal ratio, using comparative methods and theory. Stomatal ratio, defined
29 as the ratio of upper to lower stomatal density, impacts how plants 'eat' (i.e. as-
30 similate CO_2 from the atmosphere via photosynthesis). Physiological experiments
31 and biophysical theory demonstrate that amphistomatous leaves, those that have
32 equal stomatal densities on both upper and lower surfaces, maximize photosynthetic
33 rate by minimizing the distance between substomatal cavities and chloroplasts, fa-
34 cilitating rapid CO_2 diffusion [11, 12, 13, 14]. Hence, nearly all plants should be
35 amphistomatous to maximize photosynthesis, yet paradoxically up to 90% of plant
36 species in some communities are hypostomatous [15, 16, 17, 18], meaning that most
37 stomata are on the lower surface. In rare cases, most stomata are on the upper sur-
38 face (hyperstomy). I use upper and lower rather than abaxial and adaxial, because
39 the former applies to 'upside-down' (i.e. resupinate) leaves. Stomatal ratio is a quan-
40 titative metric that describes continuous variation between hypo- and hyperstomy.

41 Multiple lines of evidence indicate selection on stomatal ratio, but there is little
42 consensus on the adaptive significance. Stomatal ratio varies widely, but nonran-
43 domly [15, 17, 11, 19, 20, 21] and evolves rapidly in some taxa, possibly due to
44 selection [22, 23, 24]. Several environmental and anatomical factors have been hy-
45 pothesized to favour amphistomy (Table 1). The mechanistic details and literature
46 underlying these hypotheses and predictions are described in Text S1. The prepon-
47 derance of hypostomy almost certainly reflects a cost of upper stomata. For example,
48 hypostomy has evolved anew in resupinate leaves [25]. Upper stomata might be costly
49 because they increase susceptibility to foliar pathogens (e.g. rust fungi) that infect
50 through stomata [13], suggesting that stomatal ratio mediates a tradeoff between

4

51 photosynthetic rate and defence [23], but other costs have been proposed (Text S1).
52 Identifying the selective forces (i.e. fitness benefits and costs) shaping stomatal ratio
53 have been hampered by four methodological limitations. Namely, previous studies
54 were typically qualitative rather than quantitative, confined to specific geographic re-
55 gions or clades, did not account for phylogenetic nonindependence, and did not take
56 into account multiple confounding factors. To overcome these limitations, I assem-
57 bled a quantitative, global, and phylogenetically extensive database that disentangles
58 correlated predictor variables (e.g. light level and leaf thickness).

59 This new dataset revealed that stomatal ratio is a multimodal trait (Fig. 1). To
60 test whether the observed pattern is consistent with constraint, I modified previous
61 evolutionary process models to accommodate bounded traits like stomatal ratio. Fit-
62 ting this model to the data indicates that stomatal ratio is highly constrained by a
63 rugged adaptive landscape with multiple selective regimes (for discussion of selective
64 regimes, see [26, 27, 5]). This led me to evaluate whether selection is sufficient to
65 account for inferred constraints using theoretical and empirical approaches. First, I
66 constructed a simple cost-benefit model consistent with the underlying physics and
67 a minimum of additional assumptions. This model indicates that distinct peaks in
68 the adaptive landscape can result from selective constraints, even when the under-
69 lying environmental gradients are smooth. In contrast, a review of the literature
70 does not support a large role for genetic, developmental, and functional constraints.
71 Finally, phylogenetic multiple regression identifies life history evolution as the pri-
72 mary selective agent underlying peak shifts, but anatomical and climatic factors are
73 also important. By merging theory and data, this study adduces compelling new
74 evidence that selection is the primary constraint on phenotypic evolution, at least
75 for stomatal ratio. There is no reason to believe this trait is exceptional among func-

5

76 tional traits, and hence the inferences drawn here could be generalizable to many

77 other phenotypes that exhibit similar patterns indicative of evolutionary constraint.

Results

Stomatal ratio evolution is constrained by multiple selective regimes

81 I compiled a new, global dataset from 25 previously published studies (Text S2)

82 containing trait data (stomatal ratio and leaf thickness) on 599 species across 94

83 plant families; the dataset with trait and climate data comprised a 552 species subset

84 covering 90 families. The most striking feature of the data is that stomatal ratio (SR)

85 is highly multimodal (Fig. 1), with apparent modes at 0 (hypostomatous), ≈ 0.5

86 (amphistomatous), and 1 (hyperstomatous). Note that here I am reporting stomatal

87 ratio as the ratio of upper density to total density so that the distinct hypo- and

88 hyperstomatous modes can be seen. Stomatal ratio does not conform to a nonmodal,

89 uniform distribution (Komologrov-Smirnov test, $D = 0.433$, $P = 1.11 \times 10^{-15}$),

90 even after removing all hypostomatous (SR $= 0$) species (K-S test, $D = 0.293$,

91 $P = 1.33 \times 10^{-15}$). The data are also inconsistent with a unimodal, truncated

92 exponential distribution bounded by 0 and 1 (K-S test, $D = 0.429$, $P = 1.11 \times 10^{-15}$).

93 In contrast, the distribution of stomatal ratio values across species is consistent

94 with an evolutionary process model that includes constraints imposed by multiple

95 selective regimes, indicating a rugged adaptive landscape. Although the results pre-

96 sented in this section only identify constraint, not necessarily selective constraint,

6

97 I use selective regime because evidence in the following sections indicates that se-

98 lection is the primary constraint. To infer regimes, I augmented a commonly used

99 model of selective regimes, the Ornstein-Uhlenbeck process [28], to account for traits

100 like SR that are bounded by 0 and 1 (see Materials and Methods and Text S3 for

101 further detail and mathematical derivation). Under a bounded Ornstein-Uhlenbeck

102 process model, the stationary distribution of stomatal ratio (or any proportion trait)

103 r follows a Beta distribution:

$$f(r) = \frac{r^{2\phi\theta-1}(1-r)^{2\phi(1-\theta)-1}}{B(2\phi\theta, 2\phi(1-\theta))} \tag{1}$$

104 B($\cdot$) refers to the Beta function. A selective regime at stationarity is characterized

105 by two parameters, a long-run average or 'optimum' in the adaptive landscape, θ,

106 and a precision, ϕ, around the optimum. Greater values of ϕ produce distributions

107 that are more tightly constrained around the optimum.

108 If a trait evolves on an adaptive landscape with multiple peaks, then a model

109 with multiple selective regimes should fit the data better than a model with a single

110 regime [27, 5]. I used finite mixture model analysis (Text S4) to estimate the number

111 of selective regimes. This approach differs from conceptually similar methods, but

112 can be applied to non-Gaussian traits like SR (see [29, 30] for alternative methods

113 with Gaussian traits). I inferred three selective regimes (Table 2), but note that the

114 mapping between modes and regimes is not always one-to-one. In particular, one

115 regime produces modes at both 0 and 1 (Fig. S1). Nevertheless, the data clearly

116 support the large number of hypostomatous (SR = 0) species as a distinct mode

7

117 (Fig. S1). There was also strong support for an amphistomatous regime (compare

118 Fig. S1A to Fig. S1B). Finally, the best-supported model also included a small mode

119 for hyperstomatous species and a separate, smaller regime for species intermediate

120 between hypo- and amphistomy (Fig. S1C).

121 The same general pattern seen at the global scale – multiple selective regimes lead-

122 ing to distinct modes – is recapitulated within nine of ten families best-represented in

123 the global dataset (Fig. 2). Two regimes are supported in most (8 of 9) multi-regime

124 families, except Asteraceae, in which three regimes are favoured (Fig. 2A). In one

125 family, Rubiaceae, all species were inferred as members of a hypostomatous regime.

126 In all mutli-regime families except Poaceae, there are distinct regimes associated with

127 hypo- and amphistomy; in Poaceae, there are hyper- and amphistomous regimes in-

128 stead (Fig. 2E). However, the hyperstomatous species of Poaceae in this study may

129 not be representative of family since they are wetland specialists in the genus *Spartina*

130 [31]. Generally, the internal (i.e. amphistomatous) mode is closely centered around

131 0.5, as predicted from biophysical theory [11, 13], except in in the Rosaceae, where

132 the inferred optimum is closer to 0.25. Although I was unable to account for phyloge-

133 netic nonindependence in these analyses (see Materials and Methods), that a similar

134 pattern – species are either amphistomatous or hypo/hyperstomatous, but rarely in-

135 termediate – emerges independently in multiple families indicates the conclusions are

136 unlikely to change qualitatively once fully phylogenetic methods can be extended to

137 bounded traits. In summary, the apparent pattern of constraint on stomatal ratio is

138 strikingly similar across multiple disparate families and at a global scale, suggesting

139 convergent evolution because of shared phenotypic constraint.

8

Selection is sufficient to accommodate constraint

I analyzed a simple cost-benefit model of stomatal ratio to ask whether selection is sufficient to account for apparent phenotypic constraint. Not surprisingly, selection favours greater stomatal ratio (S_{fit}) as the fitness benefit of greater photosynthesis increases relative to the cost of upper stomata (Fig. 3A-C), but the shape of the function is highly sensitive to one parameter in the model, σ^2. In particular, the adaptive landscape goes from being smooth when σ^2 is high to rugged when σ^2 is low (Fig. 3D-F). When the landscape is smooth, intermediate phenotypes between complete hypostomy and amphistomy are best when the benefit:cost ratio itself is intermediate. In contrast, when the landscape is rugged, intermediates are universally less fit than either of the boundary phenotypes. In a rugged landscape, as the benefit:cost ratio decreases there is a sudden shift from amphistomy being favoured to hypostomy being favoured. The dearth of species with intermediate SR in nature, especially within families, therefore suggests that the adaptive landscape for stomatal ratio is generally rugged. Numerical simulations based on smooth variation in the benefit:cost ratio indicate that the simple, yet realistic assumptions of this model are sufficient to generate qualitatively similar patterns of multimodality to those seen in nature (Fig. 3G-H).

Growth form, leaf thickness, and precipitation shape stomatal ratio evolution

If stomatal ratio is strongly associated with other traits or climatic factors, especially if there are compelling *a priori* hypotheses (Table 1) supporting such associations,

162 then it suggests that trait variation is shaped by selection. Phylogenetic multiple

163 regression consistently identified growth form and, to a lesser extent, leaf thickness

164 and precipitation as the best predictors of stomatal ratio (Table 3). Amphistomy

165 was strongly associated with fast growth forms (herbaceous plants), whereas hypos-

166 tomy was most common in slower growing shrubs and trees (Fig. 4). As predicted

167 by biophysical theory [11, 13], thicker leaves also tended to be amphistomatous, al-

168 though the correlation was weak (Fig. S2A). Finally, amphistomy was more common

169 in dry environments, whereas hypo/hyperstomy were associated with higher precip-

170 itation (Fig. S2B). Elevation and leaf area index, a proxy for open habitat, were

171 not significantly associated with stomatal ratio in this dataset (Table 3). In single

172 regressions, amphistomy was more common more open environments, as in previous

173 studies [12, 18, 19, 21], but this correlation was not significant after precipitation

174 was factored into multiple regression (precipitation and leaf area index are positively

175 correlated).

Discussion

177 Phenotypic evolution is often constrained, but the relative role of selective versus

178 nonselective constraints is unclear. This study posits that multimodal traits reveal

179 distinct peaks of high fitness in a rugged adaptive landscape. Hence, the prevalence

180 of certain phenotypes and the dearth of others directly reflects selective constraints

181 on phenotypic evolution. Evidence from a new, global dataset clearly shows that

182 stomatal ratio is a multimodal trait (Fig. 1) and that multimodality has evolved

183 repeatedly in land plants (Fig. 2). These patterns are difficult to reconcile with

184 models omitting constraint, but are consistent with a rugged adaptive landscape

10

185 comprised of multiple selective regimes (Table 2). A simple cost-benefit model of

186 stomatal ratio shows that selection is a sufficient explanation, particularly when the

187 underlying adaptive landscape is predominantly rugged. Adaptive evolution from

188 one peak in the landscape to another (i.e. hypo- to amphistomy or *vice versa*)

189 appears to be primarily driven by growth form, suggesting that the fitness benefit

190 of amphistomy – faster diffusion of CO_2 to chloroplasts – is greatest in species with

191 'fast' life histories.

Multimodality implies constraint on the macroevolutionary adaptive landscape

194 Just as water is only found as ice, liquid, and steam, despite continuous variation

195 in temperature, stomatal ratio comes in partially discrete clusters corresponding

196 to hypo-, amphi-, and hyperstomy, but less often intermediate (Fig. 1). In fact,

197 the modes identified here correspond remarkably with traditional botanical classi-

198 fications [32], suggesting that these workers recognized the pattern even without

199 quantitative analyses. The multimodal pattern in the dataset cannot be explained

200 by an evolutionary process model neglecting constraint (Text S3). However, appar-

201 ent clustering could occur by systematic underrepresentation of intermediate trait

202 values [33] or nonrandom taxon sampling. It is highly improbable that intermediate

203 phenotypes exist at greater frequency in nature but are rarely reported, as most

204 studies have no *a priori* hypothesis about stomatal ratio in their study organisms.

205 If anything, by omitting many studies that report only qualitative data, I might

206 have enriched the frequency of intermediate phenotypes, as these are the most likely

207 to be reported quantitatively. Nonrandom taxon sampling, without accounting for

11

phylogeny, could also give the appearance of multimodality. To give an extreme example, if there had been a single transition from hypo- to amphistomy followed by stasis, then sampling the tips of the phylogeny would produce a multimodal pattern with apparently strong statistical support, even though it only represents a single evolutionary event. Methodological limitations prevented me from fully accounting for phylogeny (see Materials and Methods), but the fact that multimodality reappears in multiple distantly-related families (Fig. 2) makes nonrandom taxon sampling alone an unlikely explanation, though it might accentuate the pattern. Future work is needed to extend regime-inference methods [27, 29, 30] to non-Gaussian traits, as this study begins to do with a new evolutionary process model for proportion traits.

Selection is the most likely explanation for phenotypic constraint

In principle, constraint could reflect a mix of selective, genetic, developmental, and functional factors [7]. However, the preponderance of available theory and data on stomatal ratio suggests selection is responsible for most if not all of the phenotypic constraint. Genetic, developmental, and functional constraints cannot explain the dearth of intermediate phenotypes because intermediates are genetically accessible as well as developmentally and functionally possible. The appropriate mutations to generate intermediate phenotypes occur spontaneously during mutagenesis [34], segregate among natural populations [35, 36, 37, 23], and are fixed between closely related species [38, 24].

In contrast, the cost-benefit model presented here shows that with a small number

12

of realistic, evidence-based assumptions, selection is sufficient to accommodate the data and helps clarify why discrete modes form even when the underlying environmental gradients are smooth (environmental gradients need not be smooth, but it is unnecessary to assume otherwise). Stomata are often distributed equally on both surfaces (amphistomy) because this arrangement optimizes photosynthetic rate. This was an assumption of the model based on biophysical theory [11, 13]. More often, all stomata are on the lower surface because the costs of upper stomata outweigh the benefits. A dearth of intermediates between hypo- and amphistomy occurs when the landscape is rugged, making these phenotypes often fall in a fitness valley. However, the best mixture model includes a small peak of these intermediates (Table 2, Fig. S1). This suggests that although the adaptive landscape is constrained and often rugged, it may shift from rugged to smooth over macroevolutionary time. However, the fact that most species, especially within families (Fig. 2), cluster around particular modes suggests that the landscape is predominantly rugged. Finally, the small number of hyperstomatous species indicates that there are occasionally situations in which upper stomata are favoured, such as in aquatic plants or those with unusual epidermal or spongy mesophyll anatomy.

Life history, more than anatomy and climate, determines stomatal ratio

Nonrandom association between stomatal ratio, other ecologically important traits, and climate also supports a significant role for selection in shaping trait evolution. To my knowledge, this is the first study to rigorously demonstrate a strong association between growth form and stomatal ratio, although it had been suggested by

13

earlier ecological surveys [15, 39]. Two hypotheses that might explain the relation-ship between growth form and stomatal ratio are: 1) herbaceous plants have shorter leaf lifespans [40], requiring higher photosynthetic rates to pay their construction costs in a shorter time [41]; 2) herbaceous plants have faster life histories, leading to stronger selection on high growth rates, mediated in part by higher leaf-level pho-tosynthetic rate [42]. That the relationship between stomatal ratio and whole-plant lifespan holds within herbaceous (annuals vs. perennials) and woody (shrubs vs. trees), supports the second hypothesis (selection on faster life history favours am-phistomy). Although this hypothesis requires further testing, if correct, it implies remarkably strong selection on leaf-level photosynthesis, as the photosynthetic ad-vantage of amphistomy over hypostomy is only a few percent in a typical herbaceous leaf [11].

Surprisingly, I found little evidence supporting the most common adaptive expla-nation for amphistomy, that thicker leaves 'need' stomata on both sides to facilitate CO_2 diffusion [11]. In actuality, support for this hypothesis is mixed (Text S1), espe-cially when phylogenetic nonindependence is taken into account [43, 39] (but see [44]). It is now clear why previous studies came to different conclusions: thicker leaves do tend to be amphistomatous, even once phylogeny is accounted for, but the trend is weak (Fig. S2A). Less powerful studies than this one could easily have failed to de-tect a significant relationship. Hence, leaf thickness, by constraining CO_2 diffusion, imposes selection for amphistomy. I also found that amphistomy was more common in plants from low precipitation environments. For a given stomatal conductance, which is proportional to evaporative water loss, amphistomy improves water-use ef-ficiency by increasing photosynthetic rate [11], suggesting a plausible mechanism for selection on amphistomy in dry environments. Although low precipitation was cor-

14

related with habitat openness, measured using leaf area index, multiple phylogenetic regression indicated that precipitation was causal, in contrast to previous studies [18, 21]. These studies used finer scale (plant-level) descriptions of light environment that might have been missed by the coarser, satellite-based measurements of canopy cover used here. Alternatively, patterns at the global scale might differ from those within particular families or biomes. Finally, I was unable to test the effects of leaf orientation and stomatal packing on stomatal ratio, though these are likely to be important factors in many plants [20]. The evidence from this and previous studies shows that stomatal ratio is an ecologically relevant functional trait that could be valuable in physiological ecological and evolution [45].

That many ecologically important traits, like stomatal ratio, cluster around particular values but not others suggests pervasive constraint on phenotypic evolution. How can we seek a general explanation for this pattern when any particular instance requires specific mechanistic and ecological knowledge about a focal trait? For example, the emerging evidence from this and other recent studies on stomatal ratio (see especially [23]) is that peaks of high fitness are constrained by a tradeoff between photosynthetic rate and defence against foliar pathogens that preferentially infect though upper stomata. In particular, the cost-benefit model analyzed here predicts that even a small change in the fitness costs or benefits are sufficient to shift fitness peaks into qualitatively different selective regimes. If it is generally true that multimodal traits are associated with rapid regime shifts, then one way forward is to look for signatures of such shifts in closely-related species that sit astride different regimes. For example, one signature of regime shifts could be the presence of quantitative trait loci large enough to pass over valleys separating fitness peaks. Consistent with this, [24] recently identified two large effect loci that together are

15

capable of making a hypostomatous leaf amphistomatous, perhaps suggesting that these loci enabled a regime shift. Integrating comparative biology, mechanistic studies of organismal function, and the genetics of adaptation, as this and others studies [46] have begun to do, points to a general approach for evaluating the common features of macroevolutionary adaptive landscapes and, hence, the role of selection in constraining phenotypic evolution.

Materials and Methods

Assembling a comparative data set

Stomatal ratio and leaf thickness I collected quantitative data on stomatal ratio and leaf thickness from previously published studies (see Text S2 for full list of sources). These data are spread across a large and diverse literature, including functional ecology, taxonomy, agriculture, and physiology. Hence, neither a standardized nor exhaustive search was possible. I started by using Web of Knowledge to locate studies that cited seminal papers on the adaptive significance of amphistomy, specifically [11] and [12]. Once I found a paper with data, I examined papers that cited those ones. Finally, I found additional data sources in comprehensive reviews of plant anatomy [47, 32, 48]. For all data papers, I recorded the mean leaf thickness, abaxial (lower) and adaxial (upper) stomatal density for each species. Where only ranges were given, I used the midpoint. If the study included a treatment, I collected only data from the control treatment. If studies measured both juvenile and adult leaves, I used only adult leaves (no study reported only juvenile leaves). Usually data were given in a table, but occasionally I used ImageJ [49] to extract data

16

325 from figures or contacted authors for data. I only included data from studies that
326 intentionally examined both surfaces for stomata; I excluded data from studies that
327 described species categorically as "hypostomatous", or "amphistomatous", or "hyper-
328 stomatous". Excluding qualitative data was necessary because there is no standard
329 definition of "amphistomy" – it has sometimes been used to describe species that
330 have approximately equal densities on each side [11] and at other times for species
331 that have any stomata on the both surfaces [16, 15].

332 **Climate and elevation**   Based on the *a priori* hypotheses, I extracted data on
333 mean annual precipitation (average 1950 – 2000), elevation (Worldclim [50]), and
334 light environment (average leaf area index between 1982 – 1998 based on remote
335 sensing [51]). For light environment, I used a satellite indicator of leaf area index, the
336 number of leaf layers between the ground and top of the canopy. Lower leaf area index
337 is interpreted as a more open light environment. The strength of these global data
338 sources is that I was able to obtain data for every species from the same dataset. A
339 limitation of these data is that even the highest resolution ($\approx$ 1 km) data might miss
340 important temporal and microsite variation. I discuss these limitations in light of the
341 findings in the Discussion. For climate and elevation, geographic coordinates for each
342 species are needed. For this, I downloaded all georeferenced herbarium specimens
343 for a given species from GBIF (last accessed Jan 15–18, 2015) using the occ_search
344 function in rgbif [52]. I filtered out or manually edited clearly erroneous locations (e.g.
345 lat = 0 or lon = 0 or where lat and lon were clearly reversed). The mean and median
346 number of GBIF georeferenced occurrences per species was 737 and 194, respectively.
347 I calculated the trimmed-mean (10% trim) mean annual precipitation, elevation, and
348 leaf area index to further remove specimens well outside the species' range, possibly

17

349 because they were, say, misidentified, cultivated, or improperly georeferenced.

350 **Growth Form**   I partitioned species by growth form into the following categories:
351 trees, small trees/shrubs, shrubs, and herbaceous species (forbs and grasses). Herba-
352 ceous species were further subdivided into annuals, biennials, and perennials. Species
353 that were variable or intermediate (e.g. annual/biennial, annual/perennial, bien-
354 nial/perennial, or annual/biennial/perennial) were classified as 'biennial'. Subshrubs
355 with some woody growth were lumped with perennials rather than shrubs. Where
356 possible, I obtained growth form data from associated data papers. When this infor-
357 mation was not given, I used regional floras, supplemented by online trait databases
358 such as USDA Plants [53] and Encyclopedia of Life [54]. When these sources were
359 unavailable or ambiguous for a given species, I checked the primary taxonomic liter-
360 ature by searching the species name in Google Scholar.

361 **Taxonomic name resolution**   I submitted taxonomic names in the database to
362 the Taxonomic Name Resolution Service (TNRS) [55]. I used names given by TNRS
363 when it returned an accepted name or synonym with overall score greater than
364 0.97 (scores are between 0 to 1). I scrutinized names where TNRS deemed the
365 name illegitimate, gave no opinion, or was otherwise ambiguous. At that point, I
366 consulted additional plant taxonomic repositories: The Plant List [56], International
367 Plant Names Index [57], and the Euro+Med PlantBase [58]. When no accepted
368 names were identified, I used original name given by the authors. For two very
369 recent papers [59, 60], I used the names given by those authors.

Pattern to process: connecting multimodality to phenotypic constraint

372 Comparative methods often infer constraint by comparing the fit of evolutionary
373 process models with and without constraint. Constraint, usually interpreted as a se-
374 lective regime, is typically modelled as an Ornstein-Uhlenbeck process [28, 27, 5], but
375 this model is inappropriate for proportion traits like stomatal ratio. I therefore devel-
376 oped a new evolutionary process model that is analogous to an Ornstein-Uhlenbeck
377 process except that traits are bounded by 0 and 1. A full description of model
378 assumptions and a derivation of the stationary distribution under a given selective
379 regime are available in Text S3. The key result is that a trait evolving under a single
380 selective regime should conform to a Beta distribution at stationarity.

381 Multimodality suggests the presence of multiple selective regimes associated with
382 different modes. I tested for multiple regimes using a conceptually similar but some-
383 what different approach than previous studies. Current methods for inferring mul-
384 tiple selective regimes are in their infancy [27, 29, 30] and cannot yet accommodate
385 Beta-distributed traits because I could not obtain a general solution to the stochastic
386 differential equation in Text S3. Future work is needed to develop numerical meth-
387 ods, such as Approximate Bayesian Computation [61], to integrate the bounded
388 Ornstein-Uhlenbeck process model elaborated here into existing statistical frame-
389 works for multi-regime inference. However, a few lines of reasoning I discuss below
390 indicate that the main conclusions of this study are robust.

391 I used finite mixture models to infer the number of selective regimes shaping
392 stomatal ratio evolution (see [6] for a similar approach). That is, I assume the current

19

³⁹³ distribution of trait values across species can be represented as a mixture of multiple

³⁹⁴ selective regimes at stationarity, each of which is modelled as a Beta-distributed

³⁹⁵ variable. To fit models, I used an expectation-maximization algorithm to find the

³⁹⁶ maximum likelihood mixture model from the data. A complete derivation of the

³⁹⁷ likelihood function and a description of the fitting algorithm are given in Text S4. R

³⁹⁸ code to implement the algorithm is available on Dryad [62]. I selected the best model

³⁹⁹ using the more conservative Bayesian Information Criterion (BIC) to compensate for

⁴⁰⁰ the fact that I am not accounting for phylogenetic nonindependence in this analysis

⁴⁰¹ (see below). I accepted models with an additional selective regime if they decreased

⁴⁰² BIC by 2 or more. By fitting the data to the stationary distribution, I implicitly

⁴⁰³ assume that evolution is sufficiently rapid to ignore phylogenetic signal. Numerical

⁴⁰⁴ simulations of the diffusion indicate that the transitory distribution is also Beta (data

⁴⁰⁵ not shown), meaning that evidence for multiple regimes (i.e. a better fit of a mixture

⁴⁰⁶ model with multiple Beta components) cannot be an artifact of transitory behaviour

⁴⁰⁷ within a single regime. I also tested for multiple regimes within families where there

⁴⁰⁸ was sufficient data ($n \geq 15$). Ten families met this criterion. For each family, I

⁴⁰⁹ compared the fit of mixtures with $k = 1, 2,$ or 3 regimes, accepting models with an

⁴¹⁰ additional regime if they decreased BIC by 2 or more. Further, I rejected additional

⁴¹¹ regimes supported by BIC if one of those regimes contained fewer than 3 species

⁴¹² (this affected Poaceae and Salicaceae). Although testing for multiple regimes within

⁴¹³ families using the stationary distribution is an imperfect substitute for fitting the

⁴¹⁴ process model to the entire tree, it is nevertheless informative. If multiple regimes

⁴¹⁵ are found repeatedly in disparate families, this provides compelling evidence for

⁴¹⁶ convergent evolution because of phenotypic constraints imposed by similar adaptive

⁴¹⁷ landscapes.

20

Is selection sufficient to account for multimodality?

In this section, I use theory to ask under what conditions selection can explain the rugged adaptive landscape implied by fitting the evolutionary process model to the data. First, I ask whether a model with simple fitness costs and benefits of upper stomata produces multiple fitness peaks (Text S1 discusses the fitness benefits and costs associated with stomatal ratio). Next, I examine whether such a landscape generates a trait distribution that qualitatively resembles the data, even when the underlying environmental gradients are smooth. I specifically focus on the pattern observed within families, where there was generally one mode of amphistomatous species and another mode of hypostomatous species (hyperstomatous in the case of Poaceae). I also opted to tradeoff the precision of a biophysical diffusion model for a more general, albeit realistic, model with fewer parameters. Hence, the cost-benefit model of stomatal ratio is true to the underlying physics but otherwise not strongly dependent on specific assumptions. Future work will be needed to test if this more general model is consistent with mechanistic biophysical models. The symbols used in the model are summarized in Table 4.

I model selection on the logit of stomatal ratio (upper:total), which I denote $S = \text{logit}(SR) = \log\big(SR/(1-SR)\big)$, so that feasible trait variation (SR is constrained from 0 to 1) is continuous and unbounded. Fitness as a function of stomatal ratio depends on the difference between the benefits ($f(S)$) minus the costs ($g(S)$). Therefore, fitness as a function of stomatal ratio is:

$$W(S) = 1 + f(S) - g(S) \tag{2}$$

21

439 Based on biophysical theory [11, 13], I assume that there is an intermediate op-
440 timal stomatal ratio (S_{opt}) at which photosynthetic rate is maximized. Above and
441 below that optimum, photosynthetic rate decreases, which I modelled as a Gaussian
442 function:

$$f(S) = B_{\text{max}}e^{-\frac{(S-S_{\text{opt}})^2}{2\sigma^2}} \tag{3}$$

443 B_{max} defines the maximum fitness when $S = S_{\text{opt}}$. σ^2 acts akin to a shape factor
444 when the function is viewed from a logit scale. When σ^2 is large, the benefit function
445 has an inverted-U shape. There are increasing returns to fitness of the first few upper
446 stomata, but diminishing returns to further increases in SR (Fig. 3A). In contrast,
447 when σ^2 is small, the benefit function is more bell-shaped; the fitness benefit of the
448 first few upper stomata is large, but with diminishing returns (Fig. 3C).

449 I assumed a linear cost (e.g. increased susceptibility to foliar pathogens [23]) for
450 each additional upper stomate. The total cost as a function of stomatal ratio is the
451 product of the total stomatal density, the stomatal ratio (upper:total density), and
452 the cost per upper stomate. I define the slope of the cost function as C_{max}, which is
453 equal to the total stomatal density times the cost per upper stomate:

$$h(SR) = C_{\text{max}}SR \tag{4}$$

454 On a logit scale, the total cost asymptotically approaches C_{max}:

$$g(S) = \frac{C_{\max}}{1 + e^{-S}} \tag{5}$$

If more were known about the cost of having upper stomata, a more realistic model could be constructed. Without such knowledge, I believe it is judicious to start with the simplest model that makes few assumptions and therefore could apply to a large number of particular underlying mechanisms. Substituting Eqs 3 and 5 into Eq 2, fitness as a function of S is:

$$W(S) = 1 + B_{\max} e^{-\frac{(S - S_{\text{opt}})^2}{2\sigma^2}} - \frac{C_{\max}}{1 + e^{-S}} \tag{6}$$

Note that if the cost function were applied to lower rather than upper stomata, as might be the case for specialized taxa such as aquatic plants, then one could obtain the same results, except that hyper- rather than hypostomy would prevail, as in the Poaceae data. The fitness function is maximized where the marginal benefit of the next upper stomate is equal to the marginal cost:

$$\frac{df(S)}{dS} = \frac{dg(S)}{dS} \tag{7}$$

I did not obtain an analytical solution, so instead I used the optim function in R [63] to numerically solve for the stomatal ratio that maximized fitness (S_{fit}) under varying ratios of fitness cost ($C_{\max}$) to benefit ($B_{\max}$). I tuned the benefit:cost ratio by fixing $B_{\max}$ to 1 and varying $C_{\max}$ between 0.01 and 100. I also varied the shape factor σ^2 between 0.1 and 10, which appeared to capture the full range of relevant model behaviour. For all numerical solutions, I assumed that the optimal

23

471 stomatal ratio for photosynthesis was 0.5, hence $S_{\mathrm{opt}} = 0$ on a logit scale. Next,

472 I generated hypothetical trait distributions under a scenario where the benefit:cost

473 ratio varies uniformly from 10^{-2} to 10^2. I solved for S_{fit} with 10^4 evenly spaced

474 values of $B_{\max} : C_{\max}$ under low, medium, and high values of σ^2. R code for finding

475 numerical solutions is available from Dryad [62].

Testing adaptive hypotheses for stomatal ratio using phylogenetic regression

478 I tested for an association between stomatal ratio, leaf thickness, mean annual pre-

479 cipitation, elevation, leaf area index, and growth form using type 2 phylogenetic

480 ANOVA with both categorical (Growth form) and continuous (e.g. leaf thickness)

481 predictor variables. For this analysis I quantified stomatal ratio as min(upper den-

482 sity, lower density):max(upper density, lower density). In this form, stomatal ratio

483 equals 1 when the densities on each surface are the same, and goes to 0 as the distri-

484 bution become more asymmetrical (hypostomy or hyperstomy). Note that this form

485 differs from what I use in analyzing multimodality because I wanted to specifically

486 test which factors favour the phososynthetically optimal distribution (amphistomy)

487 versus suboptimal distributions (either hypo- or hyperstomy). I accounted for phy-

488 logeny using a Phylomatic [64] megatree for this relatively large and phylogenet-

489 ically extensive dataset. To examine whether results were robust to phylogenetic

490 correction, I analyzed the data using three methods: Brownian motion (high phy-

491 logenetic signal), Pagel's λ (intermediate phylogenetic signal), and no phylogenetic

492 signal (normal ANOVA). For the intermediate signal model, I estimated Pagel's λ

493 using maximum likelihood. Phylogenetic models were fit using phylogenetic least

494 squares in the R package 'caper' [65].The trait dataset and phylogeny used in these
495 analyses are available on Dryad [62].
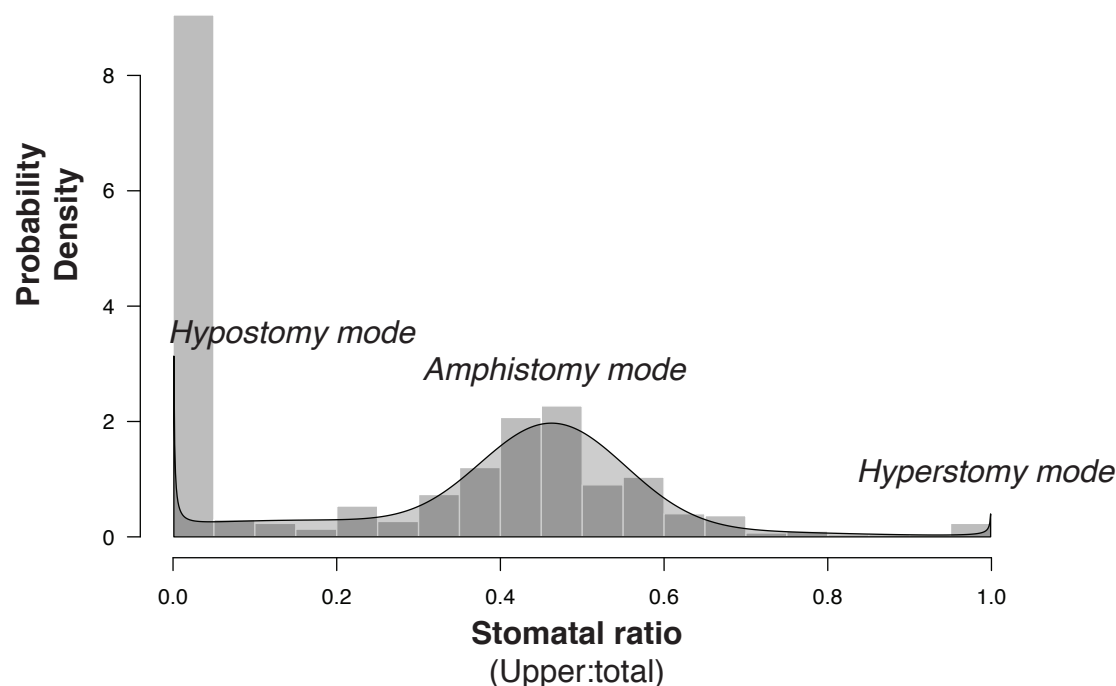
496 Acknowledgements

Figures

501

Fig. 1. Stomatal ratio is a multimodal trait. A density histogram of stomatal ratio across 599 species (light grey bars in background) displays three noticeable modes. The plurality of species are completely hypostomatous (all stomata on the lower surface; stomatal ratio equals zero). There is a smaller, broader mode of amphistomatous species (approximately equal density of stomata on upper and lower surfaces; stomatal ration equals approximately one-half). Finally, there are a small number of hyperstomatous species (all stomata on the upper surface; stomatal ratio equals one). A mixture of selective regimes (shaded grey polygon) manifests these three modes, indicating that they are real features of constrained trait evolution rather than random noise.
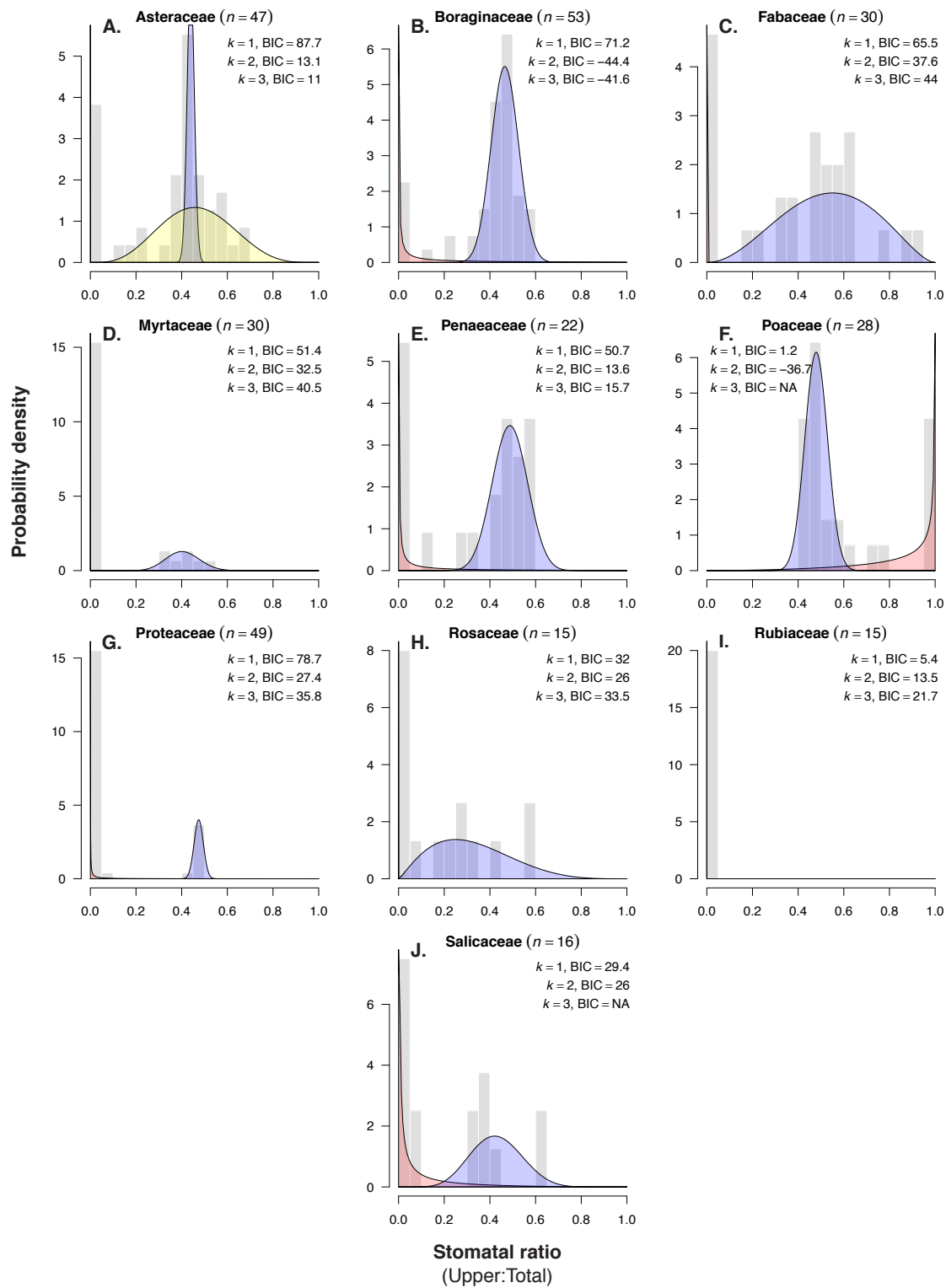
Fig. 2. Repeated evolution of multimodality suggests that the adaptive landscape is conserved across land plants. Shaded polygons of inferred regimes are plotted atop a histogram (grey bar) of stomatal ratio from a given plant family (grey bars). Note that some distributions are very narrow spikes near the origin. The title gives the family name and number of species sampled n from that family. Three regimes were inferred for Asteraceae (panel **A.**); two regimes were inferred for other families except the Rubiaceae (panels **B.-J.**). The number of regimes was inferred from information theoretic comparisons of finite mixture models with Beta-distributed components. The Bayesian Information Criterion (BIC) for models with $k = 1$, 2, and 3 components is given in the top. I accepted models with additional regimes (higher k) if they decreased BIC by two or more. In Poaceae and Salicaeae, I rejected models with $k = 3$ because some components had very low membership.
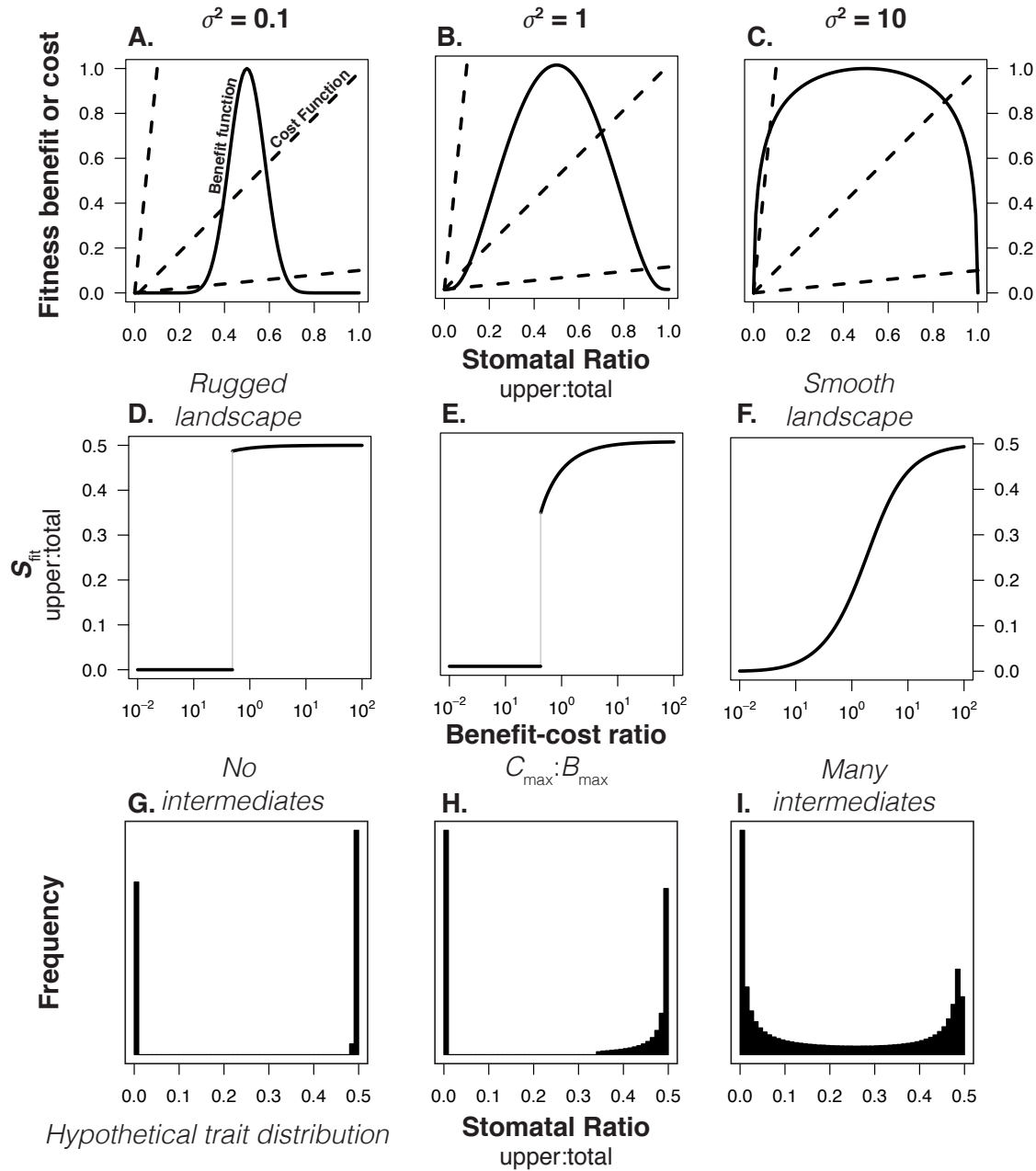
Fitness as a function of stomatal ratio

Fig. 3. Selection is sufficient to explain why intermediate phenotypes are universally unfit and the adaptive landscape is rugged. Panels **A.-C.**: In each panel, a benefit function (solid line, see Eq 3) is shown with three different cost functions (dashed line, see Eq 5). In all panels, B_{max} is fixed at 1 and three slopes of the cost function, C_{max} are illustrated: 0.1 (shallow slope), 1 (medium slope), and 10 (steep slope). The fitness benefit is always maximized when stomatal ratio is 0.5 (amphistomy), corresponding to $S_{opt} = 0$ on a logit scale. The shape factor σ^2 changes the benefit function from bell-shaped in **A.** to an inverted-U shape in **C.** Panels **D.-F.** show that the shape of the benefit function affects the topography of the adaptive landscape. Solid lines are the stomatal ratio that optimizes fitness (S_{fit}) as a function of the benefit:cost ratio ($B_{max} : C_{max}$). When the benefits are high compared to costs, amphistomy (stomatal ratio $= 0.5$) is favoured; when the costs are high, hypostomy is favoured (stomatal ratio $= 0$). However, the transition between these extremes can be abrupt when the landscape is rugged (panel **D.**) or gradual when the landscape is smooth (panel **F.**). The light gray line indicates the range of universally unfit phenotypes. Panels **G.-I.** show hypothetical trait distributions assuming that the benefit:cost ratio varies uniformly from 10^{-2} to 10^2. Histograms were generated by solving for S_{fit} with 10^4 evenly spaced values of $B_{max} : C_{max}$. Note that the trait values range from hypostomatous to amphistomatous (stomatal ratio $= 0.5$), but a mirror image distribution with hyperstomatous species would be seen if fitness costs accrued to lower stomata.
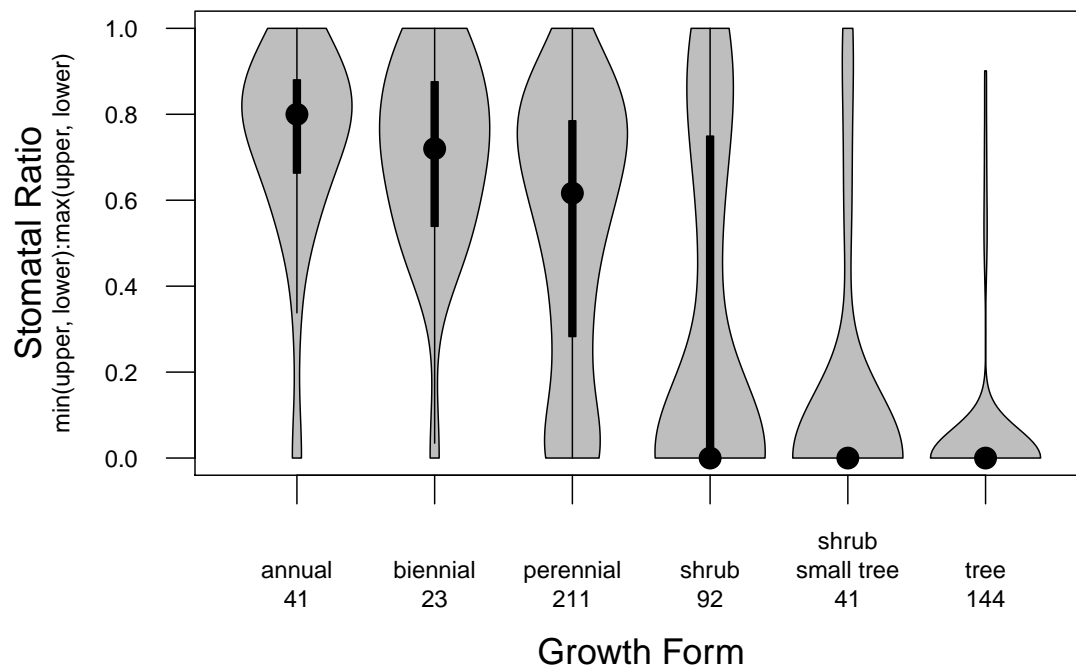
31

Fig. 4. Association between amphistomy and fast growth forms points to selection on life history shaping stomatal ratio evolution. The violin plot shows of stomatal ratio as a function of growth form across all species in the dataset. The width of the grey polygons indicates the density of data. Length of grey polygon indicate the range of the data; the point indicates the median; the thick lines indicate the 0.25 and 0.75 quantiles. Sample sizes per growth form in the dataset are given below the label.

₅₀₂ Tables

Table 1. Adaptive hypotheses and predictions for stomatal ratio. The first and second columns indicate the hypothesized ecological factors and the predicted direction of association with amphistomy, respectively. References to key studies are provided, but see Text S1 for additional detail.

Hypothesized factor	Predicted association with amphistomy	References
Leaf thickness	thicker leaves	[11]
Light	greater light intensity	[71, 12, 21]
Precipitation	lower precipitation	[17, 19]
Altitude	higher altitude	[73, 74, 75]
Growth form	herbaceous growth form	[15, 39]

Table 2. Multiple selective regimes are manifest in a multimodal trait distribution. Models with multiple components (k) corresponding to distinct selective regimes under a bounded Ornstein-Uhlenbeck process fit the data significantly better than models with a single regime (lower Bayesian Information Criterion [BIC]). In particular, the model with with three regimes is much more strongly supported than models with one or two regimes (see Fig. S1 for a visual representation of regimes). A mixture of multiple regimes, in turn, gives rise to a multimodal distribution with hypo-, amphi-, and hyperstomatous modes. For a given mixture, each of k regimes is represented as a component i parameterized by the strength of constraint (ϕ_i) around the long-term average (θ_i) and a mixture weight w_i.

k	Parameters			log-likelihood	df	BIC
1	$\phi_1 = 0.4$	$\theta_1 = 0.17$	$w_1 = 1$	-604	2	1220.9
2	$\phi_1 = 0.25$	$\theta_1 = 0.04$	$w_1 = 0.52$	-252.5	5	536.9
	$\phi_2 = 9.98$	$\theta_2 = 0.46$	$w_2 = 0.48$			
3	$\phi_1 = 0.16$	$\theta_1 = 0.02$	$w_1 = 0.47$	-237.7	8	526.6
	$\phi_2 = 17.24$	$\theta_2 = 0.47$	$w_2 = 0.38$			
	$\phi_3 = 2.04$	$\theta_3 = 0.35$	$w_3 = 0.16$			
4	$\phi_1 = 6.99$	$\theta_1 = 0$	$w_1 = 0.44$	-235.6	11	541.6
	$\phi_2 = 1.6$	$\theta_2 = 0.35$	$w_2 = 0.17$			
	$\phi_3 = 16.85$	$\theta_3 = 0.47$	$w_3 = 0.38$			
	$\phi_4 = 181.8$	$\theta_4 = 0.99$	$w_4 = 0$			

Table 3. Growth form, anatomy, and precipitation jointly determine stomatal ratio. Three models with varying levels of phylogenetic signal (Brownian motion [top], Pagel's λ [middle], and nonphylogenetic [bottom]) identify growth form, leaf thickness, and mean annual precipitation as significantly associated with stomatal ratio.

Stomatal Ratio $\sim$	df	SS	MS	F	P
Brownian Motion					
log(Leaf Thickness)	1	0.017	0.017	20.31	8.08×10^{-6}
Mean Annual Precipitation	1	0.021	0.021	24.11	1.21×10^{-6}
Elevation	1	0	0	0.08	0.78
Leaf Area Index	1	0	0	0.05	0.82
Growth Form	5	0.039	0.008	9.06	2.74×10^{-8}
Pagel's $\lambda = 0.64$					
log(Leaf Thickness)	1	0.008	0.008	24.38	1.05×10^{-6}
Mean Annual Precipitation	1	0.009	0.009	26.03	4.67×10^{-7}
Elevation	1	0	0	0.26	0.61
Leaf Area Index	1	0	0	0	1
Growth Form	5	0.027	0.005	15.52	2.77×10^{-14}
Nonphylogenetic					
log(Leaf Thickness)	1	2.376	2.376	31.67	2.94×10^{-8}
Mean Annual Precipitation	1	1.711	1.711	22.81	2.31×10^{-6}
Elevation	1	0.009	0.009	0.12	0.72
Leaf Area Index	1	0.031	0.031	0.41	0.52
Growth Form	5	15.897	3.179	42.38	7.36×10^{-37}

Table 4. Glossary of symbols used in the cost-benefit model.

Symbol	Description
SR	Stomatal ratio: ratio of upper to total stomatal density
S	logit of stomatal ratio (SR)
S_{opt}	Stomatal ratio (logit scale) that maximizes fitness benefits
B_{max}	Maximum fitness benefit when $S = S_{\mathrm{opt}}$
σ^2	Shape factor of benefit function
C_{max}	Maximum fitness cost of when all stomata are on the upper side ($SR = 1$)
S_{fit}	Stomatal ratio maximizes fitness (benefits minus costs)

References

[1] Simpson GG (1944) Tempo and mode in evolution. New York: Columbia University Press.

[2] Raduski AR, Haney EB, Igić B (2012) The expression of self-incompatibility in angiosperms is bimodal. Evolution 66: 1275–1283.

[3] Martin R, MacLarnon A (1985) Gestation period, neonatal size and maternal investment in placental mammals. Nature 313: 220–223.

[4] Fenster CB, Armbruster WS, Wilson P, Dudash MR, Thomson JD (2004) Pollination syndromes and floral specialization. Annual Review of Ecology, Evolution, and Systematics : 375–403.

[5] Mahler DL, Ingram T, Revell LJ, Losos JB (2013) Exceptional convergence on the macroevolutionary landscape in island lizard radiations. Science 341: 292–295.

[6] Scheffer M, Vergnon R, Cornelissen JHC, Hantson S, Holmgren M, et al. (2014) Why trees and shrubs but rarely trubs? Trends in Ecology & Evolution 29: 433–434.

[7] Arnold SJ (1992) Constraints on phenotypic evolution. American Naturalist 140: S85–S107.

[8] Barton N, Partridge L (2000) Limits to natural selection. BioEssays 22: 1075–1084.

[9] Gould SJ (2002) The Structure of Evolutionary Theory. Cambridge, MA: Harvard University Press.

[10] Kimball S, Gremer JR, Huxman TE, Venable DL, Angert AL (2013) Phenotypic selection favors missing trait combinations in coexisting annual plants. The American Naturalist 182: 191–207.

[11] Parkhurst DF (1978) The adaptive significance of stomatal occurrence on one or both surfaces of leaves. The Journal of Ecology 66: 367–383.

[12] Mott KA, Gibson AC, O'Leary JW (1984) The adaptive significance of amphistomatic leaves. Plant, Cell & Environment 5: 455–460.

[13] Gutschick VP (1984) Photosynthesis model for C_3 leaves incorporating CO_2 transport, propagation of radiation, and biochemistry 2. ecological and agricultural utility. Photosynthetica 18: 569–595.

[14] Parkhurst DF, Mott KA (1990) Intercellular diffusion limits to CO_2 uptake in leaves studied in air and helox. Plant Physiology 94: 1024–1032.

[15] Salisbury E (1927) On the causes and ecological significance of stomatal frequency, with special reference to the woodland flora. Philosophical Transactions of the Royal Society of London Series B 216: 1–65.

[16] Leick E (1927) Untersuchungen über den Einfluß des Lichtes auf die öffnungsweite unterseitiger und oberseitiger Stomata desselben Blattes. Jahrbücher für Wissenschaftliche Botanik 67: 771–848.

[17] Wood JG (1934) The physiology of xerophytism in Australian plants: the stomatal frequencies, transpiration and osmotic pressures of sclerophyll and

38

545   tomentose-succulent leaved plants. Journal of Ecology 22: 69–87.

546 [18] Fitter A, Peat H (1994) The ecological flora database. Journal of Ecology 82:
547   415–425.

548 [19] Gibson AC (1996) Structure-Function Relations of Warm Desert Plants. Berlin:
549   Springer-Verlag.

550 [20] Smith WK, Bell DT, Shepherd KA (1998) Associations between leaf structure,
551   orientation, and sunlight exposure in five Western Australian communities.
552   American Journal of Botany 85: 51–63.

553 [21] Jordan GJ, Carpenter RJ, Brodribb TJ (2014) Using fossil leaves as evidence
554   for open vegetation. Palaeogeography, Palaeoclimatology, Palaeoecology 395:
555   168–175.

556 [22] Howell JT (1945) Concerning stomata on leaves in *Arctostaphylos*. The Was-
557   mann Collector 6: 57–65.

558 [23] McKown AD, Guy RD, Quamme L, Klápště J, La Mantia J, et al. (2014)
559   Association genetics, geography and ecophysiology link stomatal patterning in
560   *Populus trichocarpa* with carbon gain and disease resistance trade-offs. Molec-
561   ular Ecology 23: 5771–5790.

562 [24] Muir CD, Pease JB, Moyle LC (2014) Quantitative genetic analysis indicates
563   natural selection on leaf phenotypes across wild tomato species (*Solanum* sect.
564   *Lycopersicon*; Solanaceae). Genetics 198: 1629–1643.

565 [25] Lyshede OB (2002) Comparative and functional leaf anatomy of selected Al-
566   stroemeriaceae of mainly Chilean origin. Botanical Journal of the Linnean

Society 140: 261–272.

[26] Baum DA, Larson A (1991) Adaptation reviewed: a phylogenetic methodology for studying character macroevolution. Systematic Biology 40: 1–18.

[27] Butler M, King AA (2004) Phylogenetic comparative analysis: a modeling approach for adaptive evolution. The American Naturalist 164: 683–695.

[28] Hansen TF (1997) Stabilizing selection and the comparative analysis of adaptation. Evolution 51: 1341–1351.

[29] Ingram T, Mahler DL (2013) Surface: detecting convergent evolution from comparative data by fitting ornstein-uhlenbeck models with stepwise akaike information criterion. Methods in Ecology and Evolution 4: 416–425.

[30] Uyeda JC, Harmon LJ (2014) A novel bayesian method for inferring and interpreting the dynamics of adaptive landscapes from phylogenetic comparative data. Systematic Biology 64: 902–918.

[31] Maricle BR, Koteyeva NK, Voznesenskaya EV, Thomasson JR, Edwards GE (2009) Diversity in leaf anatomy, and stomatal distribution and conductance, between salt marsh and freshwater species in the C_4 genus *Spartina* (Poaceae). New Phytologist 184: 216–233.

[32] Metcalfe CR, Chalk L (1950) Anatomy of the dicotyledons, Vols. 1 & 2. Oxford: Oxford University Press, first edition.

[33] McGlone MS, Richardson SJ, Jordan GJ, Perry GL (2015) Is there a âĂŸsuboptimalâĂŹ woody species height? a response to Scheffer et al. Trends in Ecology & Evolution 30: 4–5.

[34] Dow GJ, Bergmann DC, Berry JA (2014) An integrated model of stomatal development and leaf physiology. New Phytologist 201: 1218–1226.

[35] Hall N, Griffiths H, Corlett J, Jones H, Lynn J, et al. (2005) Relationships between water-use traits and photosynthesis in *Brassica oleracea* resolved by quantitative genetic analysis. Plant Breeding 124: 557–564.

[36] Rae AM, Ferris R, Tallis MJ, Taylor G (2006) Elucidating genomic regions determining enhanced leaf growth and delayed senescence in elevated co_2. Plant, Cell & Environment 29: 1730–1741.

[37] Gailing O, Langenfeld-Heyser R, Polle A, Finkeldey R (2008) Quantitative trait loci affecting stomatal density and growth in a quercus robur progeny: implications for the adaptation to changing environments. Global Change Biology 14: 1934–1946.

[38] Chitwood DH, Kumar R, Headland LR, Ranjan A, Covington MF, et al. (2013) A quantitative genetic basis for leaf morphology in a set of precisely defined tomato introgression lines. The Plant Cell 25: 2465–2481.

[39] Peat H, Fitter A (1994) Comparative analyses of ecological characteristics of British angiosperms. Biological Reviews 69: 95–115.

[40] Wright IJ, Reich PB, Cornelissen JH, Falster DS, Garnier E, et al. (2005) Assessing the generality of global leaf trait relationships. New Phytologist 166: 485–496.

[41] Reich PB, Wright IJ, Cavender-Bares J, Craine J, Oleksyn J, et al. (2003) The evolution of plant functional variation: traits, spectra, and strategies.

611   International Journal of Plant Sciences 164: S143–S164.

612 [42] Field C, Mooney HA (1986) The photosynthesis-nitrogen relationship in wild
613   plants. In: Givnish TJ, editor, On the Economy of Plant Form and Function,
614   Cambridge: Cambridge University Press. pp. 25–56.

615 [43] Beerling DJ, Kelly CK (1996) Evolutionary comparative analyses of the rela-
616   tionship between leaf structure and function. New Phytologist 134: 35–51.

617 [44] Muir CD, Hangarter RP, Moyle LC, Davis PA (2014) Morphological and
618   anatomical determinants of mesophyll conductance in wild relatives of tomato
619   (*Solanum* sect. *Lycopersicon*, sect. *Lycopersicoides*; solanaceae). Plant, Cell &
620   Environment 37: 1415–1426.

621 [45] Pérez-Harguindeguy N, Díaz S, Garnier E, Lavorel S, Poorter H, et al. (2013)
622   New handbook for standardised measurement of plant functional traits world-
623   wide. Australian Journal of Botany 61: 167–234.

624 [46] Heckmann D, Schulze S, Denton A, Gowik U, Westhoff P, et al. (2013) Pre-
625   dicting C_4 photosynthesis evolution: modular, individually adaptive steps on
626   a Mount Fuji fitness landscape. Cell 153: 1579–1588.

627 [47] Napp-Zinn K (1970) Anatomie des blattes. Berlin: Borntraeger.

628 [48] Metcalfe CR, Chalk L (1979) Anatomy of the dicotyledons, Vols. 1 & 2. Oxford:
629   Clarendon Press, second edition.

630 [49] Abràmoff MD, Magalhães PJ, Ram SJ (2004) Image processing with imagej.
631   Biophotonics International 11: 36–42.

[50] Hijmans RJ, Cameron SE, Parra JL, Jones PG, Jarvis A (2005) Very high resolution interpolated climate surfaces for global land areas. International Journal of Climatology 25: 1965–1978.

[51] Los SO (2010) ISLSCP II FASIR-adjusted NDVI, 1982-1998. volume 10.

[52] Chamberlain S, Ram K, Barve V, Mcglinn D (2014) rgbif: Interface to the Global Biodiversity Information Facility API. URL https://github.com/ropensci/rgbif. R package version 0.7.8.99.

[53] USDA, NRCS (2014). The plants database. Available: http://www.plants.usda.gov.

[54] (2015). Encyclopedia of Life. Available: http://www.eol.org.

[55] Boyle B, Hopkins N, Lu Z, Garay JAR, Mozzherin D, et al. (2013) The taxonomic name resolution service: an online tool for automated standardization of plant names. BMC bioinformatics 14: 16.

[56] The Plant List (2013). Version 1.1. Available: http://www.theplantlist.org/.

[57] (2015). The International Plant Names Index. Available: http://www.ipni.org.

[58] (2015). Euro+Med Plantbase. Available: http://www.emplantbase.org.

[59] Brodribb TJ, Jordan GJ, Carpenter RJ (2013) Unified changes in cell size permit coordinated leaf evolution. New Phytologist 199: 559–570.

[60] Giuliani R, Koteyeva N, Voznesenskaya E, Evans MA, Cousins AB, et al. (2013) Coordination of leaf photosynthesis, transpiration, and structural traits in rice and wild relatives (genus *Oryza*). Plant Physiology 162: 1632–1651.

43

[61] Csilléry K, Blum MG, Gaggiotti OE, François O (2010) Approximate bayesian computation (abc) in practice. Trends in Ecology & Evolution 25: 410–418.

[62] Muir CD (2015) Data from: Selection constrains phenotypic evolution in a functionally important plant trait, Dryad Digital Repository. URL http://dx.doi.org/10.5061/dryad.21bm5.

[63] R Core Team (2013) R: A Language and Environment for Statistical Computing. R Foundation for Statistical Computing, Vienna, Austria. URL http://www.R-project.org/.

[64] Webb CO, Donoghue MJ (2005) Phylomatic: tree assembly for applied phylogenetics. Molecular Ecology Notes 5: 181–183.

[65] Orme CDL, Freckleton RP, Thomas GH, Petzoldt T, Fritz SA, et al. (2013) caper: Comparative Analyses of Phylogenetics and Evolution in R. URL http://CRAN.R-project.org/package=caper. R package version 0.5.2.

[66] James SA, Bell DT (2001) Leaf morphological and anatomical characteristics of heteroblastic *Eucalyptus globulus* ssp. *globulus* (myrtaceae). Australian Journal of Botany 49: 259–269.

[67] Burrows G (2001) Comparative anatomy of the photosynthetic organs of 39 xeromorphic species from subhumid New South Wales, Australia. International Journal of Plant Sciences 162: 411–430.

[68] Williams M, Woodward FI, Baldocchi DD, Ellsworth DS (2004) CO_2 capture: Leaf to landscape. In: Smith WK, Vogelmann TC, Critchley C, editors, Photosynthetic Adaptation, New York: Springer. pp. 133–168.

[69] Goble-Garratt E, Bell D, Loneragan W (1981) Floristic and leaf structure patterns along a shallow elevational gradient. Australian Journal of Botany 29: 329–347.

[70] Poorter H, Niinemets Ü, Walter A, Fiorani F, Schurr U (2010) A method to construct dose–response curves for a wide range of environmental factors and plant traits by means of a meta-analysis of phenotypic data. Journal of Experimental Botany 61: 2043–2055.

[71] Lohr PL (1919) Untersuchungen über die Blattantomie von Alphen- und Ebenenpflanzen. Ph.D. thesis, Universität Basel.

[72] Mott KA, O'Leary JW (1984) Stomatal behavior and CO_2 exchange characteristics in amphistomatous leaves. Plant physiology 74: 47–51.

[73] Spinner H (1936) Stomates et altitude. Berichte der Schweizerischen Botanischen Gesellschaft 46: 12–27.

[74] Woodward FI (1986) Ecophysiological studies on the shrub *Vaccinium myrtillus* l. taken from a wide altitudinal range. Oecologia 70: 580–586.

[75] Körner C, Neumayer M, Menendez-Riedl SP, Smeets-Scheel A (1989) Functional morphology of mountain plants. Flora 182: 353–383.

[76] Vogel S (2012) The Life of a Leaf. Chicago: University of Chicago Press.

[77] Franks PJ, Beerling DJ (2009) Maximum leaf conductance driven by CO_2 effects on stomatal size and density over geologic time. Proceedings of the National Academy of Sciences 106: 10343–10347.

45

[78] Foster J, Smith W (1986) Influence of stomatal distribution on transpiration in low-wind environments. Plant, Cell & Environment 9: 751–759.

[79] Gates FC (1914) Winter as a factor in the xerophily of certain evergreen ericads. Botanical Gazette 57: 445–489.

[80] Pospíŝilová J, Solárová J (1984) Environmental and biological control of diffusive conductances of adaxial and abaxial leaf epidermes. Photosynthetica 18: 445–453.

[81] Smith W (1981) Temperature and water relation patterns in subalpine understory plants. Oecologia 48: 353–359.

[82] Reich P (1984) Relationships between leaf age, irradiance, leaf conductance, CO_2 exchange, and water-use efficiency in hybrid poplar. Photosynthetica 18: 445–453.

[83] Smith WK, McClean TM (1989) Adaptive relationship between leaf water repellency, stomatal distribution, and gas exchange. American Journal of Botany 76: 465–469.

[84] Boeger MRT, Gluzezak RM (2006) Adaptações estruturais de sete espécies de plantas para as condições ambientais da área de dunas de Santa Catarina, Brasil. Iheringia, Série Botânica 61: 73–82.

[85] Camargo MAB, Marenco RA (2011) Density, size and distribution of stomata in 35 rainforest tree species in Central Amazonia. Acta Amazonica 41: 205–212.

46

[86] Cooper RL, Cass DD (2003) A comparative epidermis study of the Athabasca sand dune willows (*Salix*; Salicaceae) and their putative progenitors. Canadian Journal of Botany 81: 749–754.

[87] Cooper RL, Ware JV, Cass DD (2004) Leaf thickness of *Salix* spp. (Salicaceae) from the Athabasca sand dunes of northern Saskatchewan, Canada. Canadian Journal of Botany 82: 1682–1686.

[88] Dickie J, Gasson P (1999) Comparative leaf anatomy of the Penaeaceae and its ecological implications. Botanical Journal of the Linnean Society 131: 327–351.

[89] Dunbar-Co S, Sporck MJ, Sack L (2009) Leaf trait diversification and design in seven rare taxa of the Hawaiian *Plantago* radiation. International Journal of Plant Sciences 170: 61–75.

[90] Fahmy GM (1997) Leaf anatomy and its relation to the ecophysiology of some non-succulent desert plants from Egypt. Journal of Arid Environments 36: 499–526.

[91] Fahmy GM, Hegazy AK, Ali MIA, Gomaa NH (2007) Structure-function relations of leaves in 24 species of winter and summer weeds. Global Journal of Environmental Research 1: 103–116.

[92] Fontenelle G, Costa C, Machado R (1994) Foliar anatomy and micromorphology of eleven species of *Eugenia* L.(Myrtaceae). Botanical Journal of the Linnean Society 116: 111–133.

[93] Holbrook NM, Putz F (1996) From epiphyte to tree: differences in leaf structure

and leaf water relations associated with the transition in growth form in eight species of hemiepiphytes. Plant, Cell & Environment 19: 631–642.

[94] Loranger J, Shipley B (2010) Interspecific covariation between stomatal density and other functional leaf traits in a local flora. Botany 88: 30–38.

[95] Malaisse F, Colonval-Elenkov E (1982) On the leaf anatomy of trees and shrubs of the montane evergreen foresst of Malawi and Zimbabwe. Geo-Eco-Trop 6: 139–160.

[96] Parkin J, Pearson HHW (1903) The botany of the Ceylon patanas. Journal of the Linnean Society of London, Botany 35: 430-463.

[97] Peace W, Macdonald F (1981) An investigation of the leaf anatomy, foliar mineral levels, and water relations of trees of a Sarawak forest. Biotropica : 100–109.

[98] Rao AN, Tan H (1980) Leaf structure and its ecological significance in certain mangrove plants. In: Soepadmo E, Rap AN, MacIntosh DJ, editors, Proceedings of the Asian Symposium on Mangrove Environment: Research and Management, Ardyas. pp. 183–194.

[99] Read J, Edwards C, Sanson GD, Aranwela N (2000) Relationships between sclerophylly, leaf biomechanical properties and leaf anatomy in some Australian heath and forest species. Plant Biosystems 134: 261–277.

[100] Ridge R, Loneragan W, Bell D, Colquhoun I, Kuo J (1984) Comparative studies in selected species of *Eucalyptus* used in rehabilitation of the northern Jarrah

48

760   forest, Western Australia. ii. wood and leaf anatomy. Australian Journal of
761   Botany 32: 375–386.

762 [101] Selvi F, Bigazzi M (2001) Leaf surface and anatomy in Boraginaceae tribe
763   Boragineae with respect to ecology and taxonomy. Flora 196: 269–285.

764 [102] Seshavatharam V, Srivalli M (1989) Systematic leaf anatomy of some Indian
765   mangroves. Proceedings of the Indian Academy of Sciences: Plant Sciences 99:
766   557–565.

767 [103] Sobrado M, Medina E (1980) General morphology, anatomical structure, and
768   nutrient content of sclerophyllous leaves of the âĂŸBanaâĂŹ vegetation of
769   Amazonas. Oecologia 45: 341–345.

770 [104] Hansen TF (2012) Adaptive landscapes and the comparative analysis of adap-
771   tation. In: Svensson E, Calsbeek R, editors, The Adaptive Landscape in Evo-
772   lutionary Biology, Oxford, UK: Oxford University Press. pp. 205–226.

773 [105] Pennell MW, Harmon LJ (2013) An integrative view of phylogenetic compar-
774   ative methods: connections to population genetics, community ecology, and
775   paleobiology. Annals of the New York Academy of Sciences 1289: 90–105.

776 [106] Otto SP, Day T (2007) A Biologist's Guide to Mathematical Modeling in Ecol-
777   ogy and Evolution. Princeton, New Jersey: Princeton University Press.

778 [107] Grün B, Kosmidis I, Zeileis A (2012) Extended beta regression in R: Shaken,
779   stirred, mixed, and partitioned. Journal of Statistical Software 48: 1–25.
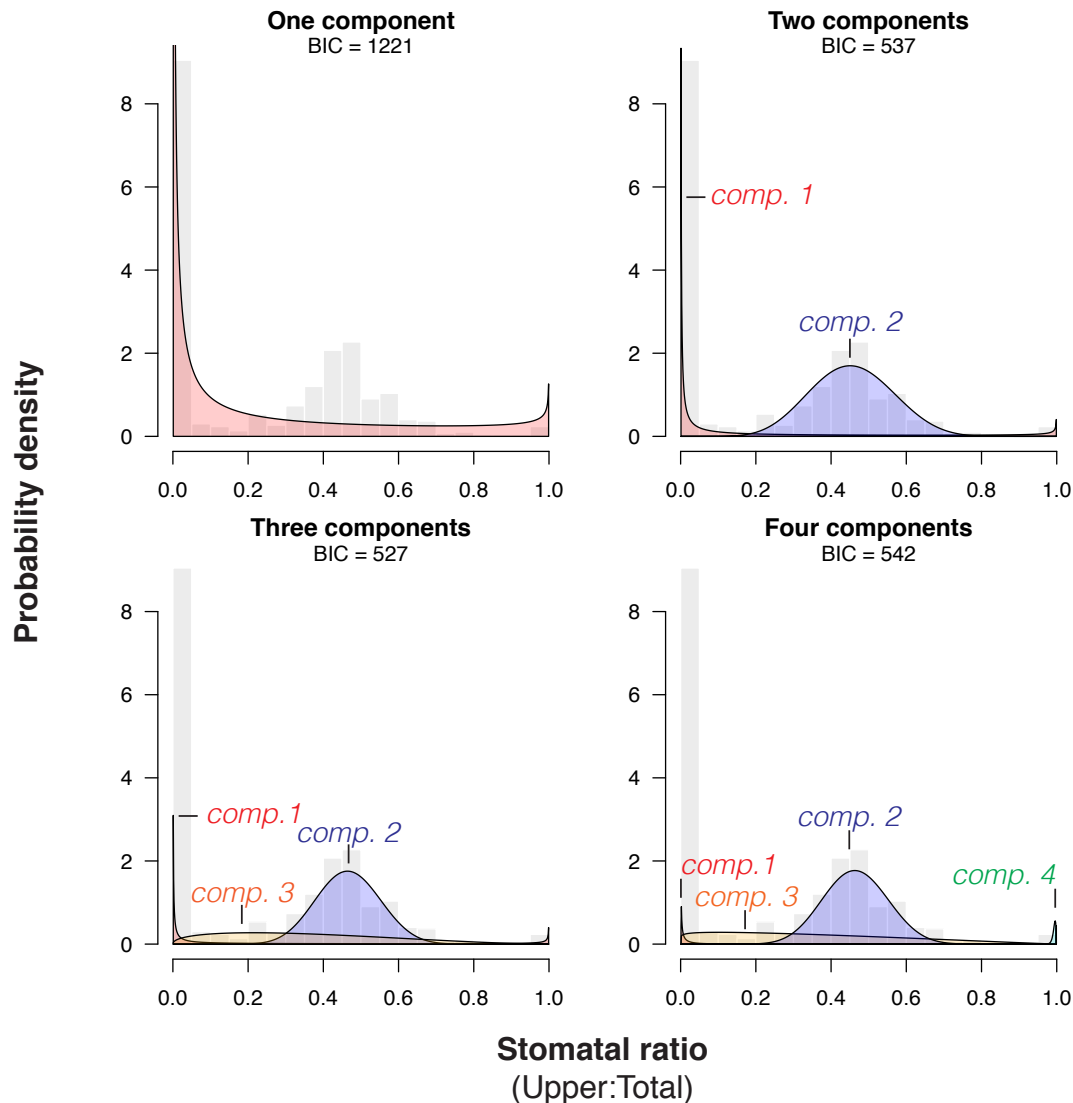
780 Supporting Information

Fig. S1. A multimodal trait distribution implies multiple selective regimes. Model selection using Bayesian Information Criterion (BIC) favoured models that were mixtures of composed multiple selective regimes. **A.** A model with one component was a poor fit because it cannot account for the large peak of amphistomatous species. **B.** A model with two components fit the data much better because it incorporates separate selective regimes for amphistomatous species (blue polygon) and hypo-/hyperstomatous species (red polygon). **C.** An additional selective regime (orange polygon) for species with stomatal ratios between 0 and 0.5 improved model fit, suggesting that intermediate phenotypes are favoured in some circumstances. **D.** Finally, a model with a fourth component (green polygon) did not significantly improve the fit (higher BIC).
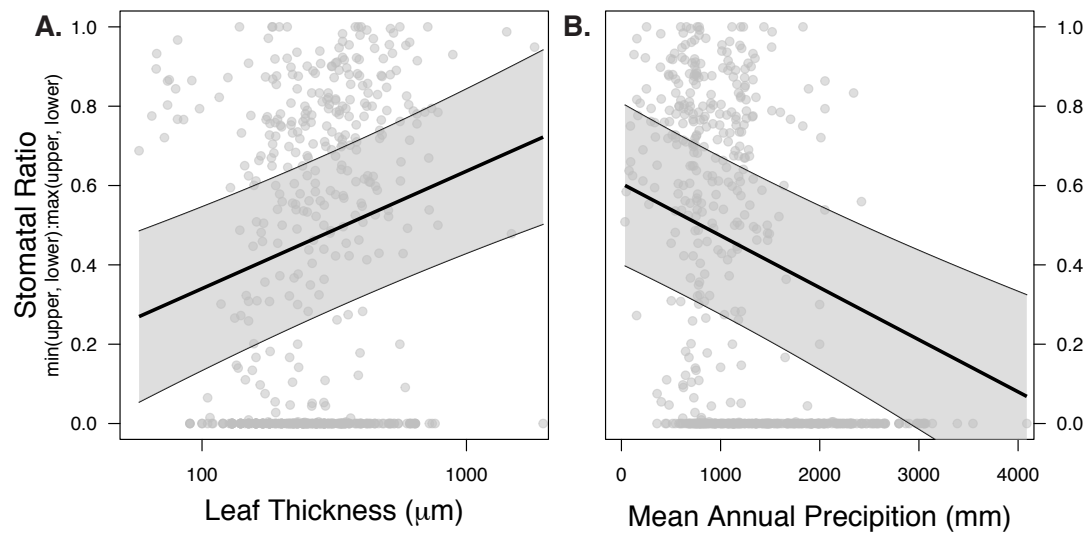
Fig. S2. Amphistomy is weakly associated with thicker leaves and drier habitats. Each point represents a species from the global dataset. The thick line and gray polygon are the median and 95% confidence intervals from the posterior distribution of predicted stomatal ratio as a function of leaf thickness based on phylogenetic regression. The fitted lines and confidence intervals are drawn with growth form set to perennial and other continuous predictor variables set to their median.

Text S1: Hypothesized benefits and costs of amphistomy

There are at least seven viable, non-mutually exclusive hypotheses for on the adaptive significance of amphistomy, five of which I evaluate here.

H1: Leaf thickness

The most widely cited and frequently tested diffusional limitation hypothesis is that amphistomy is adaptive in thick leaves. Models [11, 13] and experiments [14] demonstrate that the path length from substomatal cavities to chloroplasts can impose a large constraint on photosynthesis, especially when leaf thickness exceeds approximately 300 μm. Several studies have found a positive correlation between leaf thickness and amphistomy [11, 20, 66, 67, 68, 59, 44], but the evidence is equivocal [69, 12, 43].

H2: Light

A second hypothesis is that amphistomy is favoured in high light, open environments because CO_2 becomes more limiting at high irradiance. H1 and H2 are difficult to disentangle, and could even reinforce one another, because leaf thickness increases under high irradiance [70]. However, several studies have argued that the light environment, rather than leaf thickness, is the primary factor affecting selection on amphistomy [19, 71, 18, 12, 20, 21].

H3: Precipitation

Wood [17] observed that amphistomy was common in Australian deserts. Although amphistomy is sometimes common in dry environments, most studies conclude that precipitation is indirectly correlated with amphistomy because drier habitats also tend to be more open [19, 21]. Nevertheless, the fact that amphistomy can increase water-use efficiency [11, 72] suggests that it might be favoured in dry habitats, independent of other factors.

H4: Altitude

Anatomical surveys demonstrate that amphistomy is sometimes more common in high elevation communities compared to nearby low elevation communities [73, 74, 75], possibly because lower CO_2 partial pressures place a greater premium on efficient diffusion. However, this hypothesis is complicated by the fact that diffusion coefficients are higher at elevation because the air is thinner [76], meaning that CO_2 diffusion could actually be less limiting.

H5: Growth form

Independent of leaf anatomy and the abiotic environment, the strength of selection on photosynthetic rate might be stronger among certain growth forms (e.g. forbs vs. trees) because of their different life history strategies. Salisbury (1927) noted qualitatively that herbs tended to amphistomatous, an observation later confirmed by Peat and Fitter (1994). However, other reviews have argued that stomatal ratio

54

820 is not closely connected with any particular growth form [32, 12].

821 Two hypotheses I have not considered because of methodological limitations are

822 that amphistomy is associated with vertically-oriented, isobilateral leaves [32] and

823 that amphistomy, by doubling the conductive leaf surface area, relieves a constraint

824 the stomatal size-density tradeoff [77, 59]. I did not have sufficient, reliable informa-

825 tion on leaf orientation and guard cell size to evaluate these hypotheses.

826 Costs of upper stomata

827 This study reaffirms at a global scale that most species are hypostomatous. The

828 most parsimonious explanation for the preponderance of hypostomy is that there

829 is cost to having stomata on the upper surface of the leaf. A fitness cost associ-

830 ated with increased evaporation [78] cannot explain the dearth of stomata on the

831 upper leaf surface, though this explanation occasionally appears in the literature

832 [79]. In fact, amphistomy is common in some dry habitats [17, 11, 19, 20] and am-

833 phistomatous plants can be functionally hypostomatous when stressed by regulating

834 stomatal aperture differentially on each surface [80, 81, 82, 72]. Although amphis-

835 tomatous plants can be functionally hypostomatous, the reverse is not true. Hence,

836 anatomical amphistomy should be favoured whenever the capacity to be functionally

837 amphistomatous is advantageous.

838 Besides evaporation, several fitness costs have been suggested, including decreased

839 water-use efficiency of amphistomy in large leaves [11], photodamage to guard cell

840 chloroplasts (W.K. Smith, pers. comm.), occlusion of upper stomata by water block-

841 age [83], and increased susceptibility to foliar pathogens [13]. Increased evaporation

55

842 is an unlikely explanation since so many desert species are anatomically amphis-

843 tomatous (see above), but to my knowledge, most other hypotheses have not been

844 rigorously tested. However, [23] showed that adaxial (upper) stomata pore area, but

845 not abaxial (lower) pore area, was strongly correlated with susceptibility to a rust

846 pathogen. Hence, the pathogen susceptibility hypothesis is best supported by the

847 current data.

Text S2: Data Sources

1. Boeger and Gluzezak 2006 [84]

2. Brodribb *et al.* 2013 [59]

3. Camargo and Marenco 2011 [85]

4. Cooper and Cass 2003 [86]; Cooper *et al.* 2004 [87]

5. Dickie and Gasson 1999 [88]

6. Dunbar-Co *et al.* 2009 [89]

7. Fahmy 1997 [90]

8. Fahmy *et al.* 2007 [91]

9. Fontenelle *et al.* 1994 [92]

10. Giuliani *et al.* 2013 [60]

11. Holbrook and Putz 1996 [93]

12. Körner *et al.* 1989 [75]

13. Lohr 1919 [71]

14. Loranger and Shipley 2010 [94]

15. Malaisse and Colonval-Elenkov 1982 [95]

16. Maricle *et al.* 2009 [31]

17. Muir *et al.* 2014 [44]

18. Parkin and Pearson 1903 [96]

19. Peace and MacDonald 1981 [97]

20. Rao and Tan 1980 [98]

21. Reed *et al.* 2000 [99]

22. Ridge *et al.* 1984 [100]

23. Selvi and Bigazzi 2001 [101]

24. Seshavatharam and Srivalli 1989 [102]

25. Sobrado and Medina 1980 [103]

Text S3: An evolutionary process model for proportion traits

Making evolutionary sense of a biological pattern requires an underlying process model to provide the theoretical foundation on which data analysis rests. A powerful approach in macroevolution involves modelling trait evolution on adaptive landscapes where the peaks of high fitness evolve with or without constraint [28, 104, 105]. If models with constraint describe the data better than those without, then there is compelling evidence that the adaptive landscape is shaped by some combination of selective, genetic, functional, or developmental constraints. Furthermore, the adaptive landscape may change under multiple selective regimes, meaning that a trait is best described by a mixture of distributions, each generated under separate selective regimes [27, 29, 30]. Current evolutionary process models such as Brownian motion and Ornstein-Uhlenbeck assume that traits follow a Gaussian distribution, but this is clearly inappropriate for traits like stomatal ratio. In this text, I modify previous evolutionary process models to accommodate proportion traits and derive the expected pattern given adaptive landscapes that are constrained versus those that are unconstrained. This model provides a strong theoretical foundation for the model-based statistical inference described in Text S4. A glossary of symbols used in this text are provided in Table S1.

In both models with and without constraint, I assume that *total* stomatal density follows a random walk over macroevolutionary time, though the exact process is irrelevant here. Imagine for a set area (A_{leaf}) of leaf (e.g. 1 μm^2) there are $N_T(t) = A_{\text{leaf}}D_T(t) = A_{\text{leaf}}(D_U(t) + D_L(t))$, where $N_T(t)$ is the total number of stomata in

59

Table S1. Glossary of symbols used in process models of stomatal trait evolution.

Symbol	Description
r	Stomatal ratio: ratio of upper to total stomatal density
N_T, N_U, N_L	Number of stomata in a focal leaf area A_L
	The total number N_T is the sum of upper N_U and lower N_L stomata
D_T, D_U, D_L	Density of stomata in total, upper, and lower surfaces
A_{leaf}	Focal leaf area
ν	Diffusion coefficient of stomatal ratio
θ	Long-run average stomatal ratio
α	Return rate to long-run average ratio
ϕ	Defined as $\nu\alpha$
$M_{\delta x}$	Drift function of stomatal ratio r in diffusion approximation
$V_{\delta x}$	Diffusion function of stomatal ratio r in diffusion approximation

897 that area at time t. Total stomatal number $N_T(t)$ is the sum of upper $(N_U(t))$

898 and lower $(N_L(t))$ stomata. Let $\Delta N_{T,t} = N_T(t+1) - N_T(t)$ be the change in total

899 stomatal number that must be made up of changes in upper stomata, lower stomata,

900 or some combination of both. I assume that the contribution to $\Delta N_{T,t}$ from upper

901 and lower stomata is proportional to their density. For reasons explained below, I

902 define $\nu = N_T(t+1)$ as the total stomata at time $t+1$. The transition rate u_{ij} from

903 $N_U = i$ upper stomata at time t to $N_U = j$ upper stomata at time $t+1$ is binomially

904 distributed with a rate determined by the stomatal ratio r:

$$u_{ij} = \binom{\nu}{j} r^j (1-r)^{\nu-j} \quad j \in \{0, 1, 2, \ldots, \nu\} \tag{S1}$$

905 Note that stomatal ratio here is defined as the proportion of upper stomata, $r =$

906 $N_U/(N_U + N_L) = N_U/N_T = N_U/\nu$. The mean and variance of stomatal ratio in the

907 next time step is therefore:

$$\mu(r) = \mathbb{E}\left[\frac{N_U}{\nu}\right] = r \tag{S2}$$

$$\sigma^2(r) = \mathbb{E}\left[\left(\frac{N_U}{\nu}\right)^2\right] - \left(\mathbb{E}\left[\frac{N_U}{\nu}\right]\right)^2 = \frac{r(1-r)}{\nu} \tag{S3}$$

908   In other words, the average stomatal ratio does not change, but the variance
909 increases each time step. When ν is large, the distribution can be approximated with
910 a normal distribution and a diffusion approximation can be used to model the long
911 term evolution of the trait. This diffusion process is analogous to Brownian motion,
912 except that the trait is bounded by 0 and 1. It is also mathematically equivalent
913 to one-locus, two-allele population genetic models of neutral evolution (see [106] for
914 a detailed derivation). I will make reference to results from this literature without
915 rigorously deriving them here. In particular, it has been shown that the stationary
916 distribution of the diffusion is:

$$f(r) = \frac{e^{A(r)}\left(c_1 \int e^{-A(r)}\mathrm{d}r + c_2\right)}{V_{\delta x}} \tag{S4}$$

917   where

$$A(r) = \int \frac{2M_{\delta x}}{V_{\delta x}}\mathrm{d}r \tag{S5}$$

$$M_{\delta x} = 0 \tag{S6}$$

$$V_{\delta x} = \frac{r(1-r)}{\nu} \tag{S7}$$

61

918 and the time scale is in units of ν^{-1}. Thus, ν can be interpreted as a diffusion

919 coefficient without necessarily specifying a genetic or developmental mechanism that

920 governs the amount of variance in stomatal ratio from one time to the next. Solving

921 for $f(r)$ without selection on stomatal ratio yields:

$$f(r) = \frac{6}{r(1-r)} \tag{S8}$$

922 Thus, without selection on stomatal ratio, most species should be hypo- or hyper-

923 stomatous (Fig. S3). Next, I modify the model to include stabilizing selection around

924 a long-run average θ, which may be interpreted as a peak in the adaptive landscape

925 under a single selective regime. This process model is analogous to an Ornstein-

926 Uhlenbeck process for a bounded trait. I again use the diffusion approximation, but

927 this time the drift and diffusion coefficients are:

$$M_{\delta x} = \alpha(\theta - r) \tag{S9}$$

$$V_{\delta x} = \frac{r(1-r)}{\nu} \tag{S10}$$

928 α is the return rate to θ. Greater values of α constrain trait variation more tightly

929 around θ. With these coefficients and setting the first constant of integration c_1 to 0

930 yields:

$$f(r) = c_2 \nu r^{2\alpha\nu\theta-1}(1-r)^{2\alpha\nu(1-\theta)-1} \tag{S11}$$

62

931   where:

$$c_2 = 1 \bigg/ \int_0^1 \nu r^{2\alpha\nu\theta-1}(1-r)^{2\alpha\nu(1-\theta)-1}dr \tag{S12}$$

$$= \frac{1}{\nu \mathrm{B}(2\alpha\nu\theta, 2\alpha\nu(1-\theta))} \tag{S13}$$

932    $\mathrm{B}(\cdot)$ is the beta function. Setting c_1 to 0 can be justified by recognizing that the

933   distribution should be symmetrical ($x = 1 - x$) when $\theta = 0.5$, which only occurs if

934    $c_1 = 0$ (S.P. Otto pers. comm.). Further, I confirmed the accuracy of the analytically-

935   derived stationary distribution using stochastic simulations (data not shown).

936   Defining $\phi = \alpha\nu$, the stationary distribution simplifies somewhat to:

$$f(r) = \frac{r^{2\phi\theta-1}(1-r)^{2\phi(1-\theta)-1}}{\mathrm{B}(2\phi\theta, 2\phi(1-\theta))} \tag{S14}$$

937   This is the $\mathrm{Beta}(\alpha, \beta)$ distribution with $\alpha = 2\phi\theta$ and $\beta = 2\phi(1 - \theta)$. Note that,

938   following standard notation, α here refers to the first shape parameter of the Beta

939   distribution, not the constraint factor of the evolutionary process model. This result

940   means that the well-known statistical properties of the Beta distribution can be

941   leveraged to understand the stationary distribution of a proportion trait under a

942   constrained adaptive landscape. For example, the Beta distribution takes on a variety

943   of shapes that begin to resemble the distribution of proportional traits like stomatal

944   ratio (Fig. S4). Hence, the evolutionary process model developed here provides

63

945 a strong theoretical justification for fitting the stomatal ratio data to a mixture of

946 Beta distributions in order to infer the selective regimes shaping this trait across plant

947 species. Although I have derived the model with stomatal ratio in mind, it should

948 be applicable to wide variety of proportional traits evolving under a constrained
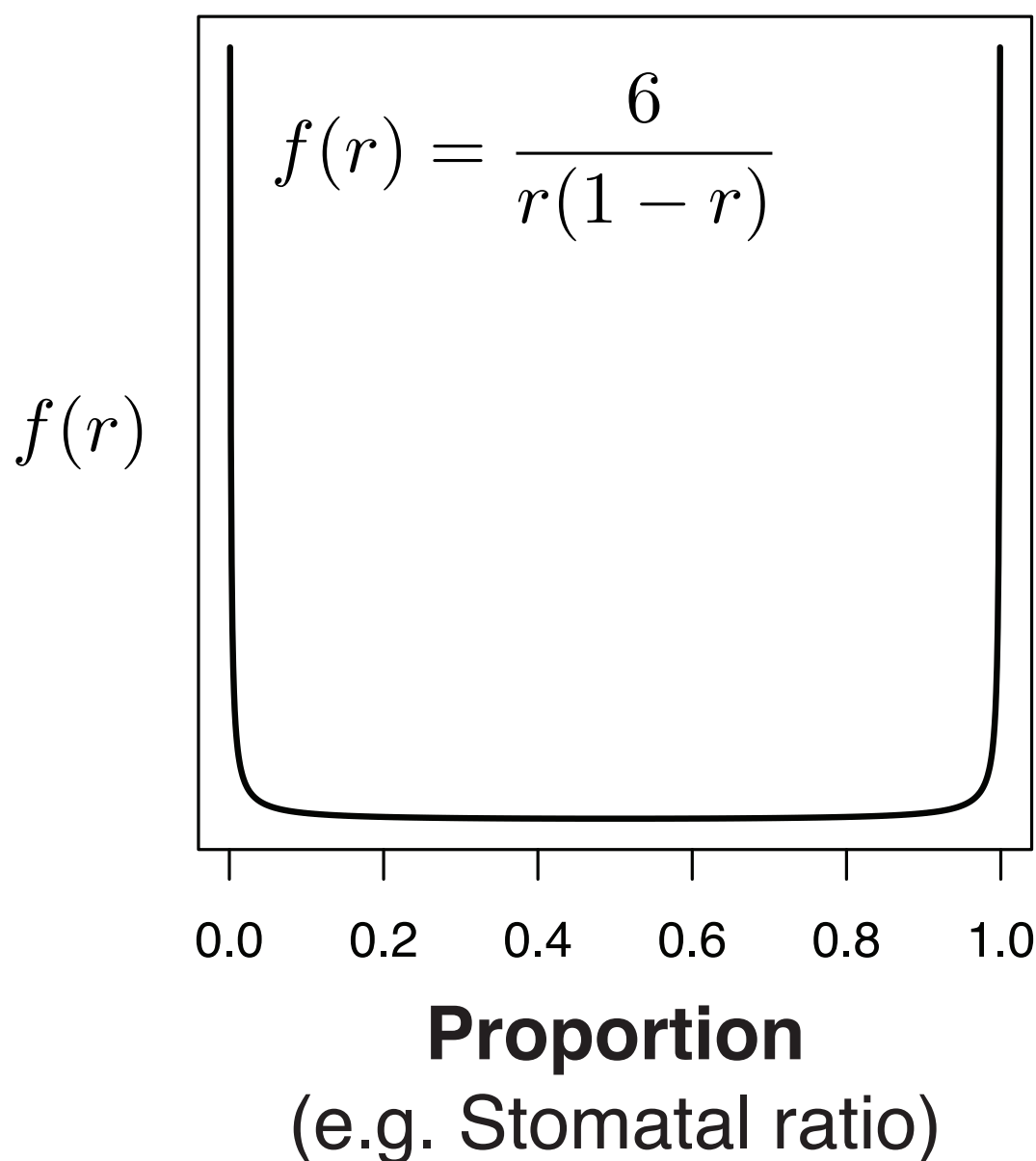
949 adaptive landscape.

Fig. S3. Without constraint, a proportion trait like stomatal ratio (r) will evolve toward a distribution in which most species are 0 or 1.
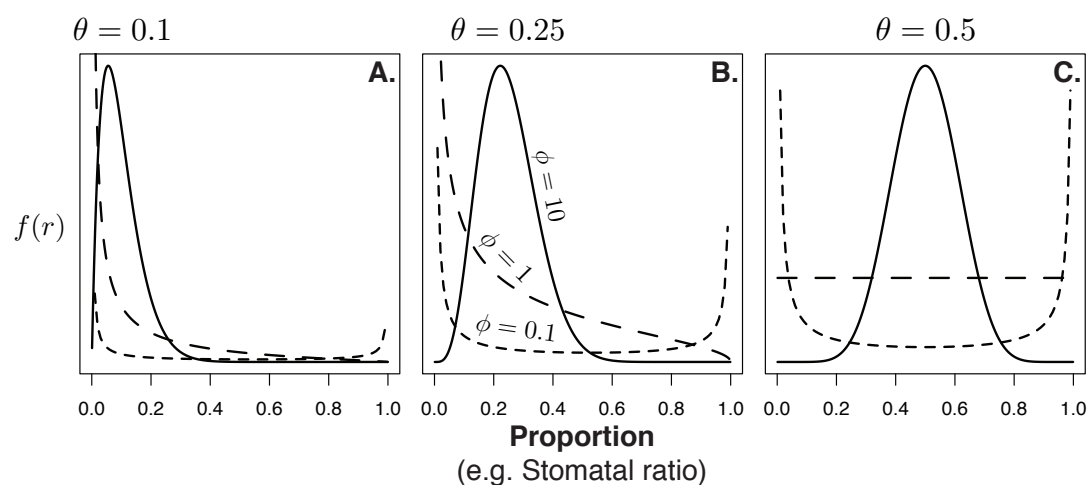
65

Fig. S4. A proportion trait like stomatal ratio evolving under a constrained adaptive landscape is Beta distributed. The Beta distribution can take on a wide variety of shapes depends on the long-run average θ and the levels of constraint ϕ (greater ϕ equals greater constraint).

Text S4: Fitting evolutionary process to pattern using finite mixture models estimated with maximum likelihood

In this paper, I infer the number of selective regimes acting on stomatal ratio by fitting a mixture of stationary distributions derived from the process model above to the data. In this section I derive the likelihood functions and describe an expectation-maximization algorithm to find the maximum likelihood mixture model given the data. R code to implement these methods is available on Dryad [62]. In general, finite mixture distributions are the summation of $k \geq 2$ mixture components (i.e. probability distributions) with density $f_i(x)$ and mixture weight w_i:

$$g(x; k) = \sum_{i=1}^{k} w_i f_i(x) \tag{S15}$$

Here the i-th mixture component has a probability density $f_i(x)$ given by the stationary distribution in Eq S14 with parameters θ_i, ϕ_i. The likelihood of a mixture distribution given k mixture components and a data vector $\boldsymbol{x}$ with sample size n is the weighted sum of the likelihoods of each component:

$$\mathcal{L}(\boldsymbol{w}, \boldsymbol{\phi}, \boldsymbol{\theta}; \boldsymbol{x}, k) = \sum_{i=1}^{k} w_i \mathcal{L}_i(\phi_i, \theta_i; \boldsymbol{x}) \tag{S16}$$

67

964   The parameter vectors $\boldsymbol{w}$, $\boldsymbol{\phi}$, and $\boldsymbol{\theta}$ are defined as:

$$\boldsymbol{w} := \{w_1, \ldots, w_k\} \tag{S17}$$

$$\boldsymbol{\phi} := \{\phi_1, \ldots, \phi_k\} \tag{S18}$$

$$\boldsymbol{\theta} := \{\theta_1, \ldots, \theta_k\} \tag{S19}$$

965   For the i-th component, the likelihood of parameters ϕ_i and θ_i given the data is
966   the product of the probability densities of each datum $(x_1, x_2, \ldots, x_n)$:

$$\mathcal{L}_i(\phi_i, \theta_i; \boldsymbol{x}) = \prod_{j=1}^{n} f_i(x_j; \phi_i, \theta_i) \tag{S20}$$

967   To obtain reasonable fits, I found it necessary to modify the likelihood to incorpo-
968   rate left- and right-censored data. This is because the stomatal ratio dataset contains
969   many 0's (all stomata are on the lower surface of the leaf) and 1's (all stomata on the
970   upper surface). Under most parameterizations of the Beta distribution, the proba-
971   bility density of 0 and 1 is ∞ or 0. I left- and right-censored the data at $x_l = 0.001$
972   and $x_r = 0.999$ as these were very close to the lowest and highest values reported
973   in the dataset (except 0 and 1), respectively. This means that any datum reported
974   as 0 was statistically interpreted as falling anywhere between 0 and 0.001. Likewise,
975   a datum reported as 1 was assumed to fall between 0.999 and 1. A reasonable in-
976   terpretation is that a stomatal ratio so close to 0 or 1 would be practically difficult
977   to measure. Biologically, a stomatal ratio less than 0.001 or greater than 0.999 are

68

indistinguishable from 0 and 1. With censoring, the likelihood of the i-th component becomes:

$$\mathcal{L}_i(\phi_i, \theta_i; \boldsymbol{x}) = \prod_{j=1}^{n} f(x; \phi_i, \theta_i)^{I_l(x) I_r(x)} F(x_l; \phi_i, \theta_i)^{1 - I_l(x)} (1 - F(x_r; \phi_i, \theta_i))^{1 - I_r(x)} \quad \text{(S21)}$$

$F(x; \phi_i, \theta_i)$ is the cumulative density function of the Beta distribution; $I_l(x)$ and $I_r(x)$ are indicator functions:

$$I_l(x) = \begin{cases} 0 & \text{if } x = x_l \\ 1 & \text{if } x \neq x_l \end{cases} \quad \text{(S22)}$$

$$I_r(x) = \begin{cases} 0 & \text{if } x = x_r \\ 1 & \text{if } x \neq x_r \end{cases} \quad \text{(S23)}$$

To find the maximum likelihood mixture distribution, I used an expectation-maximization (EM) algorithm similar to [107]. EM algorithms are particularly well-suited to fitting mixture distributions. Here, I describe the initialization, expectation (E-step), and maximization (M-step) procedure.

Initialization

The data were divided into k evenly-sized components. For example, if $k = 2$, data below the median were assigned to component 1; data above the median were

69

assigned to component 2. For each component, the initial weight was therefore $w_{i,\text{init}} = 1/k$. Within each component, I used the optim function in R to estimate the maximum likelihood parameters ($\hat{\phi}_i^{(\text{init})}$ and $\hat{\theta}_i^{(\text{init})}$) of a Beta distribution. Note that I am using parenthetical superscript to indicate the iteration of the algorithm, starting with the initial parameterization, followed by $t = 1, 2, 3, \ldots$ until the likelihood converges. The initial parameter vectors are therefore:

$$\boldsymbol{w}^{(\text{init})} := \{1/k, \ldots, 1/k\} \tag{S24}$$

$$\boldsymbol{\phi}^{(\text{init})} := \{\hat{\phi}_1^{(\text{init})}, \ldots, \hat{\phi}_k^{(\text{init})}\} \tag{S25}$$

$$\boldsymbol{\theta}^{(\text{init})} := \{\hat{\theta}_1^{(\text{init})}, \ldots, \hat{\theta}_k^{(\text{init})}\} \tag{S26}$$

Expectation

In the E-step, the expected likelihood is calculated under the parameters estimated from the previous iteration. The mixture weights are then updated and carried forward to the M-step. For the first iteration following initialization, the mixture weights $\boldsymbol{w}^{(1)}$ conditional on the initial parameterization are:

$$w_i^{(1)} = \frac{\sum_{j=1}^{N} y_{ij}^{(\text{init})}}{n} \tag{S27}$$

where $y_{ij}^{(\text{init})}$ is the probability that x_j belongs to component i given initial parameters:

70

$$y_{ij}^{(\text{init})} = \frac{w_i^{(\text{init})} f(x_j; \hat{\phi}_i^{(\text{init})}, \hat{\theta}_i^{(\text{init})})}{g(x_j; k, \boldsymbol{w}^{(\text{init})}, \boldsymbol{\phi}^{(\text{init})}, \boldsymbol{\theta}^{(\text{init})})} \tag{S28}$$

In subsequent iterations, the equations are similarly:

$$w_i^{(t+1)} = \frac{\sum_{j=1}^{N} y_{ij}^{(t)}}{N} \tag{S29}$$

$$y_{ij}^{(t)} = \frac{w_i^{(t)} f(x_j, \phi_i^{(t)}, \theta_i^{(t)})}{g(x_j; k, \boldsymbol{w}^{(t)}, \boldsymbol{\phi}^{(t)}, \boldsymbol{\theta}^{(t)})} \tag{S30}$$

Maximization

During the M-step, estimates of $\boldsymbol{\phi}$ and $\boldsymbol{\theta}$ are updated using maximum likelihood conditional on mixture weights calculated in the E-step:

$$\{\boldsymbol{\phi}^{(t+1)}, \boldsymbol{\theta}^{(t+1)}\} = \underset{\boldsymbol{\phi}, \boldsymbol{\theta}}{\arg\max} \, \mathcal{L}(\boldsymbol{\phi}, \boldsymbol{\theta}; \boldsymbol{x}, k, \boldsymbol{w}^{(t)}) \tag{S31}$$

I used the optim function in R to find the parameters that maximized the likelihood function. After the M-step, the next iteration begins at the E-step and continues until the likelihood converges to a stable value. As with other hill-climbing likelihood searches, EM does not guarantee convergence at the maximum likelihood. With the stomatal ratio data, I found that multiple initialization procedures yielded the same final parameter estimates, suggesting that the algorithm was successfully converging on the maximum likelihood solution.

71